RECCAP2 - Polar Ice Sheets

An ice sheet-to-ocean analysis of carbon stores and fluxes in Earth´s polar regions

J.L. Wadham[1,2], G. Lamarche-Gagnon[1], S. Arndt[3], E.A. Bagshaw[2], S. Garcia-Yao[4], D. Goldberg[5], J.R. Hawkings[6,1], K. Hendry[7], R.G. Hilton[8], G. Hugelius[9,10], F. M. Monteiro[2,1], J. Ramage[9,10], M. Winsborrow[1], J.R. Zondervan[11], J. Hauck[12], L. Gregor[13], S. Yasunaka[14,15], G. G. Laruelle[3], J.A. Rosentreter[16], M. Kuhn[17], Benjamin Poulter[18,19]

Affiliations

[1]*Centre for ice, Cryosphere, Carbon and Climate (iC3), Department of Geosciences, UiT The Arctic University of Norway, 9037 Tromsø, Norway*

[2]*School of Geographical Sciences, University of Bristol, UK*

[3]*BGeoSys, Department of Geosciences, Environment and Society, Université libre de Bruxelles, Belgium*

[4]*Stanford University, Vice Provost Office for Undergraduate Education, USA*

[5]*School of Geosciences, University of Edinburgh, UK*

[6]*Department of Earth and Environmental Science, University of Pennsylvania, USA*

[7]*British Antarctic Survey, Cambridge, UK*

[8]*Department of Earth Sciences, University of Oxford, UK*

[9]*Department of Physical Geography, Stockholm University, Sweden*

[10]*Bolin Centre for Climate Research, Stockholm, Sweden*

[11]*Department of Earth Sciences, University College London, UK*

[12]*Alfred Wegener Institute, Helmholtz Centre for Polar and Marine Research, Germany*

[13]*Department of Environmental Systems Science, ETH, Switzerland*

[14]*Graduate School of Science, Tokoku University, Japan*

[15]*Advanced Institute for Marine Ecosystem Change, Japan Agency for Marine-Earth Science and Technology, Japan*

[16]*Centre for Coastal Biogeochemistry, Faculty of Science and Engineering, Southern Cross University, Lismore, New South Wales, Australia.*

[17]*Department of Geography, University of British Columbia, Canada*

[18]*Spark Climate Solutions, USA*

[19]*Department of Geographical Science, University of Maryland, USA*

Corresponding authors: J.L. Wadham *(ORCID: 0000-0002-5251-7162)*: Jemma.l.wadham@uit.no, G.L. Lamarche-Gagnon: (guillaume.lamarche-gagnon@uit.no)

An edited version of this paper was published by AGU. Published (2026) American Geophysical Union:

J.L. Wadham, G. Lamarche-Gagnon, S. Arndt, E.A. Bagshaw, S. Garcia-Yao, D. Goldberg, J.R. Hawkings, K. Hendry, R.G. Hilton, G. Hugelius, F. M. Monteiro, J. Ramage, M. Winsborrow, J.R. Zondervan, J. Hauck, L. Gregor, S. Yasunaka, G. G. Laruelle, J.A. Rosentreter, M. Kuhn, Benjamin Poulter, An ice to ocean analysis of carbon stores and fluxes in Earth´s polar regions (RECCAP2: Polar Ice Sheets), Global Biogeochemical Cycles. To view the published open abstract, go to https://doi.org/10.1029/2025GB008677.

Key Points

- Polar ice sheets, land fringes and oceans host vast carbon reserves (>10,000 billion tonnes, Gt), but with high uncertainty
- Polar ice sheets and their surrounding oceans are likely net sinks for CO_2 and small sources for CH_4
- Future climate-driven changes in the polar regions have the potential to influence CO_2 and CH_4 fluxes to the atmosphere.

Abstract

The polar ice sheets, their surrounding land fringes and oceans (68 x 10^6 km^2; 13% of Earth's surface) are hot spots for carbon cycle perturbation under future climate change due to glacier retreat, rising meltwater fluxes, reduced sea ice, thawing permafrost, warming land-surfaces and increased precipitation. Here we assess carbon stored and exchanged with the atmosphere across an expansive bi-polar ice-to-ocean domain. We show that the polar regions harbour large reserves of carbon stored in sediments, rocks and the ocean which differ in their reactivity and turnover times: 5300-22,200 PgC of organic carbon and 5600-8600 PgC of inorganic carbon. These carbon reservoirs include potential reserves of marine and subglacial methane hydrate (80-570 PgC) which could become destabilised under future warming scenarios. Oceans (270-360 PgC) and ice sheets (14-96 PgC Greenland, 5000-21,000 PgC Antarctica) dominate organic carbon stores, with smaller (but regionally important) stocks found in ice sheet land fringes (13-58 PgC). Estimates of natural CO_2 and CH_4 fluxes from these polar regions to the atmosphere present high uncertainty but highlight oceanic CO_2 sinks in Greenland (-110 to -49 TgC-CO_2 a^{-1}) and in the ICE and SPSS biomes of the Southern Ocean (-480 to 55 Tg C-CO_2 a^{-1}), with potential CH_4 sources associated with the Greenland Ice Sheet. Such high uncertainty in polar carbon reservoirs and fluxes is important to resolve if future feedbacks between the polar regions, Earth's carbon cycle and climate are to be conclusively determined.

Plain language summary

Around 13% of the Earth´s surface is covered by ice sheets, their neighbouring land fringes, fjords and oceans in the polar regions. These environments are undergoing unprecedented rapid change due to warming of the atmosphere and oceans, but there is poor understanding of the amount of carbon that is stored and how it is exchanged with the atmosphere as greenhouse gases (GHGs). Our study quantifies for the first time the stores and fluxes of carbon beneath, in and around polar ice sheets, and speculates on how they might change with 21st century warming. We show vast stores of inorganic and organic carbon (>10,000 billion tonnes), and active emissions of greenhouse gases to and from the atmosphere. These regions are likely small sources of methane gas to the atmosphere and overall sinks for atmospheric CO_2. Narrowing uncertainty in these greenhouse gas emissions is important given forecast climate-driven changes in the polar regions, which have the potential to dramatically shift greenhouse gas emissions to the atmosphere.

Key Words: Polar, carbon, biogeochemistry, Antarctica, Greenland

1. Introduction: Current knowledge gaps in polar ice to ocean carbon cycles

Polar regions are hot spots for future change; amplified Arctic warming, almost four times the global mean since 1979 [*M Rantanen et al.*, 2022], is driving today´s permafrost warming and thaw [*AMAP*, 2021; *M Meredith et al.*, 2019], vegetation shifts [*AMAP*, 2021; *M Meredith et al.*, 2019], formation and growth of ice-marginal lakes [*P How et al.*, 2021] and rising freshwater fluxes from the Greenland Ice Sheet (GrIS) [*J Bamber et al.*, 2018; *K D Mankoff et al.*, 2020]. While climate warming in Antarctica has been largely limited to the Peninsular and West Antarctic region [*K A Hughes et al.*, 2021], there are reports of glacier shrinkage and rising meltwater export [*A J Cook et al.*, 2016], permafrost thaw and increased biological productivity in tundra environments [*M J Amesbury et al.*, 2017; *J Bockheim et al.*, 2013; *T A Day et al.*, 2008], which are likely to intensify and widen to other regions later this century. Furthermore, changes in ocean circulation around both ice sheets are responsible for the intrusion of warm ocean waters close to marine-terminating glaciers, driving enhanced iceberg calving, ice acceleration and thinning in Greenland, West Antarctica and some East Antarctic sectors [*T Slater et al.*, 2021].

Central to polar change are the Greenland (GrIS) and Antarctic Ice Sheets (AIS) which are an important driver of polar ocean and atmospheric circulation, energy budgets and biogeochemical cycles, via their influence on surface albedo, freshwater fluxes to oceans and land-cover types in ice-marginal areas [*M Meredith et al.*, 2019]. Despite their climate sensitivity, polar ice sheets have been excluded from global carbon cycle assessments [*P Friedlingstein et al.*, 2021]. This partly reflects a long-held belief that ice sheets do not host biologically-active stores of carbon and have negligible GHG fluxes. This view has since evolved, and ice sheets are now known to be biologically active [*A M Anesio and J Laybourn-Parry*, 2012; *M Stibal et al.*, 2012a], host sizeable stores of organic carbon [*E Hood et al.*, 2015; *J L Wadham et al.*, 2008; *K A Weitemeyer and B A Buffett*, 2006; *N Zeng*, 2003], and are physically and biogeochemically dynamic [*B J Davison et al.*, 2019; *M J Siegert et al.*, 2016]. In addition, deep subglacial sedimentary basins [*A R Aitken et al.*, 2022; *A Baranov et al.*, 2021; *G J G Paxman et al.*, 2021] are linked to groundwater discharge at ice margins [*W DeFoor et al.*, 2011; *C D Gustafson et al.*, 2022; *L C Liljedahl et al.*, 2021; *M J Siegert et al.*, 2018]. These combined factors have the potential to instigate a swath of regional to global carbon cycle feedbacks, implicating land fringes, fjords and oceans, which are sensitive to change in a warming climate [*M Meredith et al.*, 2019].

While the role of ice sheets in polar and global carbon cycles has been highlighted [*J L Wadham et al.*, 2019], it has never been placed within a wider comparative assessment of other major polar carbon pools, GHG fluxes and sensitivity to future change. This makes it challenging to evaluate the impact of polar change on the global carbon budget. Here, we quantify for the first time, stores of carbon over expansive ice-to-ocean domains of Greenland and Antarctica, including extensive land fringes, fjords and oceans. These represent what can be termed a 'boundless continuum' of environments, meaning they are intimately connected over large temporal and spatial scales and need to be treated as a continuum when assessing polar warming impacts on Earth's carbon cycle. We then quantify the present-day natural fluxes of carbon dioxide (CO_2) and methane (CH_4) to the atmosphere, evaluate current uncertainties and the potential climate-sensitivity in the 21st century. We do not account for anthropogenic (fossil) emissions in our calculations. Our assessment is a contribution

to the Global Carbon Project's second REgional Carbon Cycle Assessment and Processes study (RECCAP2), which aimed to quantify greenhouse-gas budgets, trends and drivers for 10 land, 5 ocean regions and other special regions of interest for the period 2010-2019 (land) and 1985-2018 (oceans).

2. Materials and Methods

2.1 Study area, carbon stocks and fluxes

This study covers a total area of 68 x 10^6 km^2 at both poles (c. 13% of the Earth´s surface at 510 x 10^6 km^2), and specifically: 1. Ice sheets; 2. Non-glaciated land fringes; 3. Fjords (Greenland only); and 4. Surrounding oceans (Figure 1). Ice sheets are delimited according to their present-day areas, following previous classifications. For the Southern Ocean, we considered two biomes located south of the Polar Front, between 45 and 50 °S [*J Hauck et al.*, 2023]. The Ice Biome (ICE, also referred to as the Antarctic Zone) includes >50% sea ice for part of the year and average sea surface temperatures (SSTs) of <4 °C. The Subpolar Seasonally Stratified Biome (SPSS, also termed the Polar Frontal Zone) has SSTs of <8 °C, divergent surface flow-driven upwelling around the Antarctic Polar Front, and typically has higher chlorophyll-a concentrations due to nutrient supply [*A R Fay and G A McKinley*, 2014]. For Greenland oceans, the RECCAP2 ICE-3 region [*A R Fay and G A McKinley*, 2014] was employed, and supplemented to include southern Greenland using the RECCAP2 COAST mask [*G G Laruelle et al.*, 2017] between 55 to 75 °N/10 to 60 °W, but excluding the shelf from south of 60 °N and east of 10 °W. Both of our ocean domains are influenced by the presence of ice sheets to some degree; glacial freshwater discharge influences the Southern Ocean up to latitudes north of 50 °S via iceberg drift, particularly along the Antarctic Peninsular and Ross Sea regions [*W A Dickens et al.*, 2019], and by meltwater influences on ocean circulation [*J-J Chen et al.*, 2023] and; Greenland runoff can reach 100s of kilometres offshore, e.g. Baffin Bay and the Labrador Sea [*K R Arrigo et al.*, 2017; *H Luo et al.*, 2016] and towards Iceland via the sub-polar gyre [*K Perner et al.*, 2019].

We estimated present-day carbon stocks, as organic carbon (OC) and inorganic carbon (IC) in particulate and dissolved forms, i.e. POC or SOC (Soil Organic Carbon, permafrost only) and DOC; PIC and DIC respectively. We report the summation of these data (Table 1) as: shallow OC (<1m, Equation 1); total OC (Equation 2); and total IC (Equation 3). These pools of carbon have different reactivities and are mobilized on different temporal and spatial scales, summarized in Table 1. We go on to estimate fluxes of CO_2 and CH_4 to the atmosphere across our ice-to-ocean continuum (where data was available), including OC budgets for Greenland fjords. We largely employed bottom up, data-driven estimates, since top-down estimates (e.g. via inversion models) are limited by scarcity of data in polar regions. We summarise methodologies employed to compile carbon stocks and fluxes in each of our sectors in the following sections, with full details, including uncertainty in Text S1-10.

Table 1 Equations for inorganic and organic carbon stocks in this assessment, stock descriptions and potential reactivity. GR=Greenland, ANT=Antarctica.

Equations used to calculate summed stocks

(1) $\boldsymbol{Shallow\ OC}\ (<\mathbf{1m}) = OCB_{O<1m} + OCB_{F<1m} + OC_{SG<1m} + OC_{PF<1m}$

(2) $\boldsymbol{Total\ OC} = OCB_{O<1m} + OCP_O + M_O + OCB_{F<1m} + OCP_F + DOC_{ICE} + POC_{ICE} + OC_{SG<1m} + OC_{SG>1m} + M_{SG} + OC_{PF<3m} + OC_{SR<1m} + OC_{PL} + HC$

(3) $\boldsymbol{Total\ IC} = ICB_{O<1m} + ICB_{F<1m} + ICP_O + ICP_F + IC_{SG-rocks<1m} + IC_{SR<1m} + IC_{PL}$

Term	Description	Region	Potential reactivity and impact on the atmosphere
Polar Ice Sheets			
$OC_{SG<1m}$	POC in subglacial sediments <1m (incl $OC_{SGR<1m}$)	GR, ANT	Sensitive to physical erosion and biogeochemical alteration, with potential for export to fjords and GHG emission to the atmosphere [*T Cowton et al.*, 2012; *J L Wadham et al.*, 2012]. We note that $OC_{SG<1m}$ also includes estimated subglacial OC contributions from rocks. Thus, when calculating Shallow and Total OC, we exclude the $OC_{SGR<1m}$ stock (Equations 1/2).
$OC_{SGR<1m}$ $IC_{SGR<1m}$	OC/IC in subglacial rocks <1m	GR	
$OC_{SG>1m}$	POC in subglacial sediments >1m	GR, ANT	Likely of low reactivity, with limited potential for export beyond the ice margin, but may be cycled to methane and stored as hydrate + free gas (see M_{SG}).
DOC_{ICE} , POC_{ICE}	DOC/POC in ice sheets	GR, ANT	Released in glacial meltwaters, and often highly bioavailable. Cycled in land fringes, fjords and coasts, with turnover times of days [*E Hood et al.*, 2015; *E Hood et al.*, 2009].
Land Fringes			
$OC_{SR<1m}$ and $IC_{SR<1m}$	OC/IC in surficial land fringe rocks <1m	GR, ANT	Both oxidation of exposed rock OC and sulphide oxidation/carbonate dissolution release CO_2, while silicate mineral weathering may act as a long term sink for CO_2 [*R G Hilton and A J West*, 2020; *J R Zondervan et al.*, 2023].
$OC_{PF<3m}$	SOC in permafrost <3m	GR	Soil Organic Carbon (SOC) in permafrost is sensitive to cycling by abiotic and biotic processes [*G Hugelius et al.*, 2014; *K A St. Pierre et al.*, 2019; *S Zolkos et al.*, 2018], with potential emissions of CO_2 and CH_4 to the atmosphere.
$OC_{PF<1m}$	SOC in permafrost <1m	GR, ANT	
OC_{PL} IC_{PL}	DOC/DIC in proglacial lakes	GR	DOC is sensitive to cycling by abiotic (e.g. photochemical, solubility changes) and biotic processes (e.g. vegetation changes, microbial cycling) [*J E Saros et al.*, 2015], with potential release of GHGs. DIC is linked to lake-air CO_2 exchange [*K A St. Pierre et al.*, 2019].
Deep Hydrocarbons			
HC	OC (oil and gas)	GR, ANT	Mobilised via seeps and faults [*K Andreassen et al.*, 2017; *G E Kleber et al.*, 2023; *P Serov et al.*, 2017; *K M Walter Anthony et al.*, 2012] and by extraction (i.e. oil and gas) [*F G Christiansen*, 2021], with potential for CO_2/CH_4 release to the atmosphere.
M_{SG}	Subglacial methane hydrate + free gas	ANT	Sensitive to changes in pressure and temperature, with potential to influence atmospheric GHGs if oxidative losses are <100% [*J L Wadham et al.*, 2012].
M_O	Methane hydrate in oceans	GR, ANT	Sensitive to changes in sea level/temperature, with potential to result in net CH_4 fluxes to the atmosphere, depending on oxidative losses in the ocean [*C D Ruppel and J D Kessler*, 2017].
Oceans and Fjords			
OCB_O	Benthic POC in <1m of ocean sediments	GR, ANT	Accumulates over years (glacially influenced fjords) to 100s-1000s of years and is a long-term sink for CO_2. While traditionally assumed to be unreactive, coastal POC is sensitive to disturbance and can be remineralised to CO_2, e.g. by mining, habitat degradation [*T B Atwood et al.*, 2020] and OCB can be microbially degraded [*M Ruben et al.*, 2023]..
OCB_F	Benthic POC in <1m fjord sediments	GR	
OCP_O	Pelagic DOC in oceans	GR, ANT	DOC comprises a vast diversity of molecules of differing bioavailability, cycled microbially at widely varying rates (hours to 10,000s years) [*D A Hansell and C A Carlson*, 1998; *C Lønborg et al.*, 2020] with potential for CO_2 fluxes to the atmosphere [*C Lønborg et al.*, 2020]. Can be influenced by DOC/POC fluxes from ice sheets [*E Hood et al.*, 2015].
OCP_F	Pelagic DOC+POC in fjords	GR	
ICB_O	Benthic IC in <1m ocean sediments as PIC	GR, ANT	Potential for dissolution dependent on carbonate saturation and influenced by changes in ocean chemistry and biological activity, e.g. acidification, organic matter remineralisation [*F S Freitas et al.*, 2022; *J Hauck et al.*, 2012]. This alters the ocean´s buffering capacity over 10s to 1000s of years [*T DeVries*, 2022].
ICB_F	Benthic PIC/DIC in <1m fjord sediments	GR	
ICP_O	Pelagic DIC in oceans	GR, ANT	Directly linked to ocean air-sea CO_2 exchange [*D Carroll et al.*, 2022; *F-J W Parmentier et al.*, 2017], and influenced by temperature, evaporation/precipitation, ocean circulation and biological activity (e.g. nutrient supply from ice sheets [*J L Wadham et al.*, 2019]).
ICP_F	Pelagic DIC in fjords	GR	

2.2 Polar ice sheets

2.2.1 Carbon stores We employed previous estimates of POC and DOC in both ice sheets [*E Hood et al.*, 2015]. OC reserves beneath the present-day GrIS were estimated from POC measured in silty/diamicton layers of ice cores [*P R Bierman et al.*, 2014; *A J Christ et al.*, 2021], marginal basal ice [*J A Graly et al.*, 2018; *M Stibal et al.*, 2012b; *J C Yde et al.*, 2010] and suspended sediments of glaciers in southwestern Greenland [*M P Bhatia et al.*, 2013; *T Kohler et al.*, 2017; *G Lamarche-Gagnon et al.*, 2022b; *E C Lawson et al.*, 2014; *K Vrbická et al.*, 2022], as well as estimates of subglacial rock OC ($OC_{SGR<1m}$, Section 2.3.2). Shallow POC pools (<1 m) were estimated for different sectors of the GrIS, based on expected thermal regime [*J A MacGregor et al.*, 2016], erosive behaviour [*N Maier et al.*, 2021], and using the median and interquartile range (IQR) of POC measurements. We limited our estimates of deeper sedimentary carbon stores to the palaeofluvial and impact-crater basins near Camp Century, northwest Greenland [*G J G Paxman et al.*, 2021] and warm-based sectors of the GrIS that have been estimated as "soft" [*N Maier et al.*, 2021], conservatively assuming

maximum depths of 80 m and 50 m depth respectively, which were combined with subglacial POC data (Text S1). In Antarctica, we use data from previous studies to estimate minimum/maximum estimates of the POC (<1m and > 1m) in sedimentary basins [*J L Wadham et al.*, 2019; *J L Wadham et al.*, 2012] (Text S1).

2.2.2 Carbon Fluxes Lateral OC fluxes from the GrIS employed previously reported DOC [*M G Andrews et al.*, 2018; *M P Bhatia et al.*, 2013; *K A Cameron et al.*, 2017; *A Z Csank et al.*, 2019; *J R Hawkings et al.*, 2021; *A M Kellerman et al.*, 2021; *G Lamarche-Gagnon et al.*, 2022a; *E Lawson et al.*, 2014; *A J Pain et al.*, 2020] and POC concentrations in glacial runoff [*M P Bhatia et al.*, 2013; *T Kohler et al.*, 2017; *G Lamarche-Gagnon et al.*, 2022b; *E C Lawson et al.*, 2014; *K Vrbická et al.*, 2022]. The GrIS-wide DOC flux was calculated from the product of discharge-weighted mean DOC concentrations (and standard deviations) and the 2007-2016 mean Greenland annual runoff [*J Bamber et al.*, 2018]. DOC fluxes from non-glacial rivers were taken from the literature [*A J Pain et al.*, 2020] applied to the Greenland land fringe area, or from DOC concentrations [*A Z Csank et al.*, 2019]) multiplied by the 2007-2016 annual Greenland non-glaciated runoff [*J Bamber et al.*, 2018]. For POC, we applied the median and IQR of POC concentrations (Figure S1 and S2) to the estimated GrIS suspended sediment flux [*I Overeem et al.*, 2017] (Text S2). Due to limited data, we assumed POC fluxes from non-glacial rivers were zero. We also include previously published DOC and POC fluxes associated with GrIS iceberg discharge [*J L Wadham et al.*, 2019] (Dataset S2), which were compared with OC fluxes in Greenland fjords (Dataset S2). DOC and POC fluxes associated with subglacial and iceberg discharge in Antarctica are derived from [*J L Wadham et al.*, 2019] (Dataset S2).

We calculated potential atmospheric fluxes of CH_4 and CO_2 associated with Greenland runoff arising from biogeochemical cycling at the ice sheet bed. Due to the lack of scalable measurements of CH_4 emissions from the GrIS [*J R Christiansen and C J Jørgensen*, 2018; *M Dieser et al.*, 2014; *G Lamarche-Gagnon et al.*, 2019; *A J Pain et al.*, 2021], we estimated a range of potential emissions from subglacial settings based on methane seep emissions from glacier-fed ice-marginal lakes as a "thought experiment"[*L S Brosius et al.*, 2024]), applied to 10-100% of Greenland's ablation zone (zone of net mass loss) (Text S2). For CO_2 fluxes associated with GrIS rivers, we used seasonal compilations of major ion and pH data from two well-studied catchments in western Greenland [*E A Bagshaw et al.*, 2021]), which were used to model the DIC concentrations and pCO_2 in runoff using the PHREEQC interactive model [*D Parkhurst and C A J Appelo*, 2013; *L Pötter et al.*, 2021] (Text S2, Figure S3). This allowed us to thus estimate the potential drawdown of CO_2 (i.e. ΔCO_2) into these waters as they re-equilibrate with the atmosphere proglacially. To scale our catchment estimates of ΔCO_2 to the entire GrIS and assess potential CO_2 drawdown, we used 2007-2016 GrIS runoff estimates [*J Bamber et al.*, 2018] and ΔCO_2 data from land-terminating catchments of different size from both high and low melt years (Text S2). These estimations also allowed us to calculate potential DIC fluxes from the GrIS (Figure S3). An absence of data precluded these calculations for the AIS.

2.3 Land Fringes

2.3.1 Permafrost region stocks and fluxes

Greenland SOC stocks were taken from the Northern Circumpolar Soil Carbon Database version 2 (NCSCDv2 [*G Hugelius et al.*, 2013a; *G Hugelius et al.*, 2013b] (Text S3). Antarctic permafrost SOC stocks (0-1 m) were estimated using SOC measurements from the literature, scaled up using the areal extent of different soil orders and adjusted using estimated ice-free areas for each region [*A Burton-Johnson et al.*, 2016]. The synthesis by [*J G Bockheim and N W Haus*, 2014] was used as a basis and updated with more recent SOC measurements [*C Colesie et al.*, 2014; *D W Hopkins et al.*, 2021; *C V Pires et al.*, 2017; *A Thomazini et al.*, 2015]. We report permafrost SOC stocks derived from the median and IQR of SOC contents in <1 m of permafrost for both poles, and also for <3 m of Greenland permafrost. We also provide new DOC and DIC stock estimates for Greenland proglacial lakes (Text S3, [*J R Hawkings and S B Garcia-Yoa*, 2022]), extracting Greenland lake surface data through QGreenland [*T Moon et al.*, 2021] with a high-resolution digital elevation model [*C Porter et al.*, 2018] to estimate lake volumes following [*M L Messager et al.*, 2016] and [*A J Heathcote et al.*, 2015]. DOC stocks were derived using the lake volume and mean, median and full range of DOC and DIC concentrations in Greenland lakes [*N J Anderson et al.*, 2019; *L Stolpmann et al.*, 2021] (Text S3).

CO_2 and CH_4 emissions for Greenland land fringes were estimated using a data-driven synthesis for all Arctic permafrost regions in RECCAP2 (2000-2020) [*J Ramage et al.*, 2024], applied only to ice-free Greenland areas. Areas were extracted from the Boreal Arctic Wetlands and Lakes Dataset (BAWLD). Briefly, average CO_2, CH_4 daily fluxes of the major permafrost ecosystem classes were scaled-up to their respective Greenland areal cover in BAWLD (Text S4). A similar approach was used for aquatic fluxes, with lake and river surface areas extracted from the BAWLD aquatic ecosystem dataset, and CH_4 fluxes derived from the same dataset and classified based on classes and sizes [*J Ramage et al.*, 2024]. For Greenland rivers, we used the mean-annual CO_2 flux reported for the Arctic [*S Liu et al.*, 2022], and the global mean CH_4 flux [*E H Stanley et al.*, 2016]. We compared the former with our estimates of CO_2 fluxes compiled using GrIS runoff data (Section 2.2.2). We report the mean and 95% confidence interval. Due to the small amount of permafrost and associated carbon in Antarctica, we do not calculate fluxes.

2.3.2 Surficial rock carbon stocks and fluxes

We combined rock geochemical data (USGS Rock Geochemical Database, [*USGS*, 2008]), existing global maps of surface lithology (GLiM, [*J Hartmann and N Moosdorf*, 2012], continental scale rock type abundance [*P Amiotte Suchet et al.*, 2003], and rock density data [*G E Manger*, 1963; *S Peng and J Zhang*, 2007] to project average rock OC and IC concentrations and stocks for the first 1m of bedrock in land fringes of both ice sheets ($OC/IC_{SR<1m}$, Text S3, Table S1) and in subglacial Greenland ($OC/IC_{SGR<1m}$, Section 2.2.1) following the approach of [*J R Zondervan et al.*, 2023]. We report the median and IQR of these surface rock OC and IC stocks. In terms of potential release of CO_2 from these areas, we estimated a plausible range of rock weathering rates using data from other world regions (Text S4). We compiled estimates of CO_2 release rates from previous catchment studies, considering both oxidation of petrogenic OC in rocks and sulphide oxidation of carbonate minerals as potential CO_2 release mechanisms [*R G Hilton and A J West*, 2020]. We then selected an upper and lower bound carbon oxidation yield for both petrogenic OC oxidation and sulphide weathering/carbonate dissolution (in tC km^{-2} a^{-1}) from the compiled estimates for each major rock type in ice sheet land fringes

(Table S1). Our estimates of silicate weathering rates derived from riverine ion fluxes for two catchments with the most similar climates to Greenland and Antarctica [*S Moon et al.*, 2014].

2.4 Deep hydrocarbon stocks and fluxes

We estimated deep oil and gas reserves in Greenland and Antarctica (Text S5), employing a methodology based on the IPCC energy assessment outlined in [*IPCC*, 2006] to convert barrels of oil/gas equivalent to a mass of carbon. A maximum estimate of Greenland deep oil and gas resources in on and offshore basins was sourced from [*D L Gautier et al.*, 2009], and we report the mean, 5th and 95th percentiles of data. A single minimum estimate was derived from the Greenland Resource Assessment (oil only) [*G R A D Portal*, 2022] (Table S2). For Antarctica, we employed [*J Kingston*, 1992] as a minimum estimate of barrels of oil equivalents in 21 geological provinces on continental and offshore areas, reporting the most likely hydrocarbon stock, and the 5th and 95th percentiles. A single maximum estimate was generated by the USGS assessment of undiscovered oil and gas resources in 13 Antarctic basins [*B St John*, 1986] (Table S3).

In addition, we report published model results for biogenically produced methane hydrate in East Antarctica and thermogenically-produced hydrate+free gas in West Antarctica [*J L Wadham et al.*, 2012] (See Text S5). No methane hydrate estimates exist for the GrIS. Methane hydrates stocks in polar oceans were sourced from [*K Kretschmer et al.*, 2015], estimated by extrapolation for the areas around Greenland and Antarctica, and checked against [*R H James et al.*, 2016] for the Arctic.

We estimated methane fluxes from potential onshore seepages sites in Greenland using minimum [*G Etiope et al.*, 2019] and maximum [*G E Kleber et al.*, 2023] estimates of methane fluxes from individual Arctic seeps, and multiplying them by 130 seepage sites in the GEUS petroleum seeps and stains database [*F Christiansen and J Bojesen-Koefoed*, 2021] (Text S6). Insufficient data is available to allow this in Antarctica. We also calculated the potential methane flux from Greenland offshore seeps, by scaling estimates of sea-to-atmosphere transfer of methane from the western Svalbard margin [*S Mau et al.*, 2017]) to the combined area of Greenland´s deep oil and gas geological reservoirs [*G R A D Portal*, 2022], yielding 0.008 Tg CH_4 a^{-1} (Text S6). We do not include this value in summed CH_4 fluxes from hydrocarbon seeps, due to the uncertain fate of CH_4 emission at the seafloor.

2.5 Fjords carbon stocks and fluxes

Since fjord areas around the AIS are limited, we focussed on Greenland fjords (Text S7 and S8). The total fjord surface area, water volume, and latitudinal distribution was estimated from BedMachine Greenland v3 bathymetric data [*M Morlighem et al.*, 2017]. A Greenland fjord mask was created by subtracting the extended MARgins and CATchments Segmentation (MARCATS, [*G G Laruelle et al.*, 2017]) regional Greenland mask from the ocean mask of the BedMachine data to separate the open ocean from the fjord bathymetry.

Fjord pelagic POC stocks were estimated based on latitudinal estimates of POC export, taking into account the sea ice-free period at each grid point [*H L Sørensen et al.*, 2015] (text S7 and S8). The gridded POC fluxes were then converted to POC flux profiles using the Martin curve based on the relationship constructed for Scoresby Sund, east Greenland [*M Seifert et al.*, 2019]. The resulting POC flux profiles were

then converted to POC stocks by multiplying the flux with a representative particle settling rate, integrating over the respective water column depth at each grid point and scaling by area. Fjord pelagic DIC and DOC stocks were estimated by multiplying the fjord volume with the median and IQR of observed fjord DIC/DOC concentrations [*H C Henson et al.*, 2023; *M J Hopwood et al.*, 2016; *T Horikawa et al.*, 2022; *M L Paulsen et al.*, 2017]. Limited data precluded fjord pelagic PIC stock estimations.

Fjord benthic POC stocks were derived by analytically solving the steady-state, one-dimensional conservation equation for POC in porous media under steady state conditions. The solution was parametrized and forced with representative Greenland values of surface sediment OC content, sedimentation rate, bioturbation intensity parameters, porosity and sediment density (Table S4). The analytical solution was then integrated over the first 1 m of bioturbated and non-bioturbated sediment to derive benthic POC stocks.

Fjord benthic PIC stocks were estimated from observed PIC surface sediment contents, sedimentation rate, porosity and sediment densities, and integrating the surface sediment PIC content over 1 m. The benthic DIC stock was estimated by analytically solving the steady-state, one-dimensional conservation equation for DIC in porous media, and integrating the analytical solution of the equation over the first meter of bioturbated and non-bioturbated sediment.

CO_2 and CH_4 exchange fluxes between fjord waters and the atmosphere at the present day were estimated by multiplying the median and IQR of areal CO_2 exchange rates for fjords from the RECCAP2 North America Region [*J A Rosentreter et al.*, 2023] with the surface area of Greenland fjords (Text S8, Table S6). In addition, we calculated primary productivity (PP) and POC burial in Greenland fjords by two methods: 1. using empirically-derived relationships between these fluxes and ice free periods ("ice-free period method") [*H L Sørensen et al.*, 2015] and 2. using the product of the area of marine terminating glacier (MTG)-influenced fjords and non-MTG influenced fjords (calculated from our bathmetrically-based fjord areas) and mean and standard deviation PP rates from MTG and non MTG-influenced fjords [*M J Hopwood et al.*, 2020] ("MTG method"). POC deposition fluxes and POC burial fluxes to deep fjord sediments (>1m sediment depth) were derived using a one-dimensional benthic reaction transport model (Text S7).

2.6 Ocean carbon stocks and fluxes

Pelagic DOC and DIC stocks were based on the GLODAP (Global Ocean Data Analysis Project) v2 2021 database [*S K Lauvset et al.*, 2021]. There was insufficient data coverage to calculate pelagic POC and PIC. Mean values of DIC and DOC were calculated over all locations, depths and times within the specified regions for the Southern Ocean and Greenland. The means and standard deviations (and median and IQR) of all measurements were then multiplied by total ocean volumes (based on the GEBCO 1-minute grid) to estimate stocks (Text S9). For ocean POC and PIC stocks, we employed published data of the sedimentary POC (as Mg C km^{-2}) and PIC (carbonate as %) contents of the upper 1 m of marine sediments (Table S5 and [*T B Atwood et al.*, 2020]). PIC % contents were converted to mass in the top 1m following [*T B Atwood et al.*, 2020] (Text S9). We then employed median, and IQR estimates of gridded (Greenland/Antarctic POC, Antarctic PIC) or individual datasets (Greenland PIC), and summed over the relevant areas [*A R Fay and G A McKinley*, 2014] at both poles to generate stock estimates and uncertainty.

We derived estimates of air-sea CO_2 fluxes for oceans around Greenland and Antarctica (Text S10). For Greenland, we employed pCO_2 flux estimates from two surface ocean observation-based pCO_2 products and 14 Global Ocean Biogeochemistry Models (GOBMs) from the RECCAP2 Arctic Ocean assessment [*S Yasunaka et al.*, 2023] for 1985-2018 (Table S6). For the Antarctic ICE and SPSS biomes, we drew upon estimates of air-sea exchange of CO_2 from 11 observation-based pCO_2 products and 13 GOBMs from the RECCAP2 Southern Ocean Assessment, mostly derived for 1985-2018 [*J Hauck et al.*, 2023]. The pCO_2 products fill extensive gaps in the sparse ship-based measurements of CO_2 using statistical interpolation methods (e.g. artificial neural networks). The GOBMs simulate the cycling of carbon in the ocean through physical and biogeochemical processes and were forced by atmospheric forcing fields.

3. Carbon stocks in and around ice sheets

Carbon stocks in this assessment (Figure 2, Dataset S1) cover expansive ice-to-ocean domains in Antarctica and Greenland; 62.5 and 5.8 x 10^6 km^2 respectively (Figure 1), around 13% of the Earth's surface. Total OC stores are estimated at 5276-22,019 PgC in Antarctica and 61-210 PgC in Greenland (Figure 2), where the higher Antarctic OC stock reflects both the larger study area and the presence of deep subglacial sedimentary basins which host large OC reserves. We estimate a further 5473-8411 PgC (Antarctica) and 131-197 PgC (Greenland) of inorganic carbon, dominated by benthic and pelagic sectors of the Southern Ocean (>98% of the total IC across both poles) (Figure 2). We evaluate the distribution, uncertainty and importance of these carbon stocks in the following sections, summarised in Figure 2.

3.1 Antarctic carbon stocks

3.1.1 Antarctic Ice Sheet Antarctic subglacial sedimentary basins host the largest OC stores in our assessment (4952-21,097 PgC), with small stocks in glacial ice (2.6-12 PgC, [*E Hood et al.*, 2015]) (Figures 2 and 3). The former has associated high uncertainty due to sparse data on sediment thicknesses and the unknown origin of sediments beneath the ice sheet, which might include ancient marine organic matter, ground-up rock or mixed sources [*B Gill-Olivas et al.*, 2021; *A B Michaud et al.*, 2016; *J L Wadham et al.*, 2012]. While deep subglacial OC stocks might traditionally be assumed to be unreactive and immobile, recent discoveries of active microbial populations in subglacial lakes [*B C Christner et al.*, 2014; *C L Davis et al.*, 2023], deep groundwater flow to > 1km depth in Antarctic subglacial sediments [*H A Dugan et al.*, 2022; *C D Gustafson et al.*, 2022; *J A Mikucki et al.*, 2015] and high geothermal heat fluxes in West Antarctica [*W Colgan et al.*, 2021; *C F Maule et al.*, 2005] reveal these sedimentary repositories to be biologically, hydrologically and thermally active, which has implications for carbon transport and formation of methane hydrate (Section 3.1.2).

3.1.2 Deep Hydrocarbons We report significant deep oil and gas reserves in onshore and offshore Antarctic sedimentary basins (3.7-23 PgC, [*J Kingston*, 1992; *B St John*, 1986], Table S3), amounting to 1–6.6% of global reserves (at 345 PgC [*P Friedlingstein et al.*, 2021]). High hydrocarbon potential is indicated in some sectors (e.g. Ross and Weddell Seas), but the inaccessibility of ice-covered areas limited accurate assessments. This is relevant since some sedimentary basins (e.g. Wilkes and Aurora) host thick sediments and sedimentary

bedrock, including predicted coal beds and marine hydrocarbons [*B St John*, 1986]. These oil and gas reserves, together with POC in sedimentary basins (Section 3.1.1), are likely important for methane gas hydrate formation and deep carbon mobilisation [*K Andreassen et al.*, 2017; *J L Wadham et al.*, 2012].

At present all estimations of subglacial and marine Antarctic methane hydrate reserves rely on model assessments, and poorly constrained boundary conditions drive high uncertainty (e.g. OC reactivity/content, sediment properties, geothermal fluxes, fluid migration, Figures 2 and 3). We estimate 42-480 PgC potential methane hydrate beneath the Antarctic Ice Sheet (for the most likely scenarios). In East Antarctica, where deep sediments and frozen basal conditions in some basins are likely to favour biogenic methane hydrate formation, models report highly variable methane hydrate+free gas stocks (33 PgC assuming sediments of 0.2% POC content/low reactivity and 390 PgC assuming a 1% POC content/reactivity similar to marine organic matter) [*J L Wadham et al.*, 2012]. In West Antarctica, thermogenic methane hydrate+free gas reserves have been predicted but with order of magnitude uncertainty [*J L Wadham et al.*, 2012] due to uncertain geothermally active areas and fluid flow rates (Figure 2). In support of subglacial methane generation are high methane concentrations in Antarctic subglacial lake sediment porewaters [*C L Davis et al.*, 2023; *A B Michaud et al.*, 2017] and methane seepage in the Ross Sea [*S Seabrook et al.*, 2025; *A R Thurber et al.*, 2020]. We also estimate 20-60 PgC methane hydrate in ocean sediments [*K Kretschmer et al.*, 2015], but this is likely to be an underestimate since thermogenic formation was not considered. This is supported by observations of methane hydrate offshore in the South Shetland and South Orkney Islands (e.g. Bransfield Strait), Wilkes Land margin and the Ross Sea [*M Giustiniani and U Tinivella*, 2021]. The potential marine and subglacial methane hydrate stock (63-562 PgC) is significant compared to global estimates of 500-3000 PgC [*K Kretschmer et al.*, 2015] and is important because of its potential to be destabilised by perturbation of pressure and temperature fields in both ice sheets and oceans (Section 5) [*K Andreassen et al.*, 2017; *P Serov et al.*, 2017; *K M Walter Anthony et al.*, 2012].

3.1.3 Land Fringes Land fringe permafrost and surficial rocks comprise small standing stocks of OC in Antarctica (IQR=4.6–39.2 PgC) but have order of magnitude uncertainty due to data limitations (Figure 3). Our first time estimates of Antarctic permafrost OC stocks, based on [*J G Bockheim and N W Haus*, 2014], are very low (median=0.14 PgC) and are exceeded by those in surficial rocks (median=13.8 PgC), a reflection of the small areal distribution of permafrost ecotypes (Figure 1). Areal stocks for both rock and permafrost OC (median: 9.4 kg m^{-2} and 5.6 kg m^{-2} respectively, Figure S19, Dataset S1) exceed those in ocean sediments (medians: 3.7-4.1 kg m^{-2}). Surprisingly high but uncertain IC stocks are also found in Antarctic land fringe rocks (IQR=7-245 PgC, Figure 2) which reflect 78% of the bedrock exposure identified as mixed sedimentary and metamorphic potentially bearing carbonate minerals (Table S1), which has relevance to potential CO_2 fluxes via sulphide weathering.

3.1.4 Oceans Beyond the Antarctic Ice Sheet, the Southern Ocean dominates southern polar carbon stocks (Figure 2, Dataset S1). IC dominates the marine carbon stock (median = 1417 PgC benthic PIC as marine carbonates, and 5001 PgC pelagic DIC). Around 70% of benthic PIC falls in the SPSS biome, which is

consistent with its intersection with the ′great calcite belt′ [*W M Balch et al.*, 2011] of the polar frontal zone compared with more siliceous sediments of Antarctic Zone ′opal belt′ [*Z Chase et al.*, 2015], reflecting differing planktonic assemblages and export to the deep ocean [*K M Krumhardt et al.*, 2020; *O Sachs et al.*, 2009]. Higher stocks of DIC in the SPSS biome are consistent with its larger volume (65% of DIC in the SPSS, for 65% of Southern Ocean volume), but DIC concentrations in upper ocean layers rise polewards (Figure S16) as has been reported in other studies, reflecting the importance of upwelling and cold temperatures towards the Antarctic continent [*L Gregor and N Gruber*, 2021; *Y Wu et al.*, 2019; *V E Zemskova et al.*, 2022].

Marine OC stocks are an order of magnitude smaller than IC stocks, with OC in benthic sediments (medians=77 and 110 PgC for ICE and SPSS biomes respectively) double that stored in the pelagic ocean (median=31 and 57 PgC for ICE and SPSS biomes respectively), but with low data availability in several sectors (e.g. Figure S14). We note that our PIC and POC marine stocks exclude marine benthic organisms on Antarctic and sub-Antarctic shelves, with annual carbon immobilisation estimated at up to 0.16 PgC a^{-1}, and with high potential for change with ice shelf collapse and sea ice retreat [*D K A Barnes et al.*, 2018]. As for DIC, pelagic DOC stocks are consistent with volumetric differences between the SPSS and ICE biomes. DOC concentrations in the near-surface ocean, which are characteristically low in the Antarctic high latitudes [*D A Hansell and M V Orellana*, 2021], are found in higher concentrations (>50 moles m^{-3}) than in deeper waters (<50 μmolL^{-1}, Figure S16, [*P Kähler et al.*, 1997; *H Ogawa et al.*, 1999]), where the former comprise higher fractions of younger reactive material via biological production, compared to deeper, older, more refractory DOC [*D A Hansell and C A Carlson*, 1998; *P Kähler et al.*, 1997].

Overall, marine benthic IC and OC stocks account for 28% and 8% of the estimated global <1m benthic PIC (5000 PgC [*R E Zeebe*, 2012]) and <1m benthic POC pools respectively (2322 PgC [*T B Atwood et al.*, 2020]), for a 13% contribution to a global ocean area of 361 x 10^6 km^2 [*B W Eakins and G F Sharman*, 2010]. This suggests higher burial of PIC but lower OC burial rates in our sectors of the Southern Ocean compared to other world oceans. However, both these estimates may also be influenced by low data availability. DIC and DOC stocks account for 13% of total ocean stocks (at 662 Pg DOC [*D A Hansell*, 2013] and 37,200 Pg DIC [*L Keppler et al.*, 2020]), which is in line with our Antarctic oceanic region being 13% of global ocean volume (1335 x 10^6 km^3, [*B W Eakins and G F Sharman*, 2010]).

3.2 Greenland carbon stocks

There are several fundamental differences in Greenland and Antarctic ice-to-ocean domains, which impact carbon stocks. The total area considered in Greenland is approximately ten times smaller than Antarctica (Figure 1), but Greenland hosts more extensive permafrost (0.4 x 10^6 km^2, compared with 0.03 x 10^6 km^2 in Antarctica), greater proglacial lake coverage (>12,000 km^2 versus <1000 km^2 in Antarctica, [*L Gerrish et al.*, 2020]), extensive fjords, and more productive coastal oceans, as indicated by higher surface DOC concentrations (up to 180 μmolL^{-1} versus 60 μmolL^{-1} in Antarctica, Figure S16 and 17). While extensive Antarctic subglacial sedimentary basins have been reported, detection of deep sediments beneath the GrIS is patchy and there is uncertainty as to sediment depths and properties [*A D Booth et al.*, 2020; *K Christianson*

et al., 2014; *S Franke et al.*, 2020; *C Hofstede et al.*, 2018; *B Kulessa et al.*, 2017; *G J G Paxman et al.*, 2021; *F Walter et al.*, 2014].

3.2.1 Greenland Ice Sheet As in Antarctica, OC associated with subglacial sediments (14-95 PgC) is a significant proportion of total OC stocks in the region (23-45%), equal to up to c. 10% of Arctic permafrost <3m stocks ([*G Hugelius et al.*, 2014]). However, the origin of OC beneath the GrIS is poorly constrained, and particularly the degree to which ancient soil organic matter from past phases of ice sheet growth or re-advance is still preserved beneath the ice. Ice cores from cold-based regions support the presence of pre-glacial soil organic matter and vegetation beneath inland ice (millions of years, Figure S1) [*P R Bierman et al.*, 2014] and younger material (1000s years) in basal ice, at ice sheet margins and in runoff from small glacial outlets [*M P Bhatia et al.*, 2013; *E C Lawson et al.*, 2014; *E C O'Donnell et al.*, 2016; *J C Yde et al.*, 2010]. However, the low POC content of suspended particulate matter (Figure S1) in runoff from large Greenlandic outlet glaciers [*E C Lawson et al.*, 2014], despite its bioavailability and mixed age [*T Kohler et al.*, 2017; *E C Lawson et al.*, 2014], seems consistent with a predominantly lithogenic source. The uncertainty in subglacial sediment POC contents drives order of magnitude uncertainty in <1m subglacial OC stocks and overlapping estimates of OC beneath the GrIS from rock sources (IQR=1.9-14.5 PgC) and subglacial sediments which also include rock sources (IQR=4.3-20 PgC) (Figures 2 and S19). This uncertainty rises when deeper sediments are included in subglacial OC stock estimates (IQR=10-75 PgC) and reflects their unknown origin (Figure 3). The reported uncertainty in subglacial POC stocks is important, since the reactivity of subglacial OC influences its potential to be microbially cycled to methane [*M Dieser et al.*, 2014; *G Lamarche-Gagnon et al.*, 2019] or to be exported as bioavailable DOC [*M P Bhatia et al.*, 2013; *A M Kellerman et al.*, 2021; *E C Lawson et al.*, 2014; *A J Pain et al.*, 2020]. Our calculations also reveal important IC in the form of carbonate in <1m subglacial (median=22 PgC) and land fringe rocks (median=14.9 PgC). These rock carbonates have the potential to be weathered in wet-based sectors of the GrIS or in recently exposed proglacial landscapes by acidity generated by sulphide oxidation, which may result in a source of CO_2 to the atmosphere.

3.2.2 Deep Hydrocarbons Deep hydrocarbon reserves in Greenland, as for Antarctica, are poorly constrained. Assessments of oil and gas in offshore Greenland report similar estimates (mean=4.7 PgC [*D L Gautier et al.*, 2009] and 3.2 PgC [*G R A D Portal*, 2022]), despite the former excluding areas south of the Arctic circle. Some sectors (e.g. the northwest Greenland rifted margin and north Greenland shelf) fall at the high end of estimates for the whole Arctic, which contains around 13% of global undiscovered oil and gas reserves [*D L Gautier et al.*, 2009] and some western Greenland reserves have become sites of targeted exploration in recent decades [*F G Christiansen*, 2021].

We highlight the potential for deep sedimentary hydrocarbon reserves to extend beneath the ice and to be associated with mobile gas hydrates. Offshore in Greenland, we estimate 18-30 PgC of methane hydrate [*K Kretschmer et al.*, 2015], consistent with discoveries of methane hydrate and gas/fluid related features associated with deep petroleum systems via geophysical surveys in northwest, west and northeast Greenland [*D R Cox et al.*, 2020; *D R Cox et al.*, 2021; *T Nielsen et al.*, 2014; *P Reynolds et al.*, 2017]. Given high

geothermal fluxes in parts of Greenland, such as the northeast [*W Colgan et al.*, 2021; *P Reynolds et al.*, 2017; *S Rysgaard et al.*, 2018] and the presence of sedimentary rocks and/or soil organic matter in thick subglacial sediments [*A J Christ et al.*, 2021], it seems probable that methane hydrate exists beneath the GrIS. This is consistent with recent modelling studies [*G Lamarche-Gagnon et al.*, 2019], but requires field validation and detailed mechanistic modelling where boundary conditions are well constrained.

3.2.3 Land Fringes Smaller, but regionally important, stores of OC exist in Greenland land fringes: 8.7 PgC (median, as <3m permafrost = 0.01 % for the entire Arctic, [*G Hugelius et al.*, 2014]) and 3.2 PgC (median) in surficial rocks; but direct samples of these outcrops are lacking (Figure 3, Dataset S1). Greenland permafrost SOC content rises from low values in southern Greenland in isolated and sporadic permafrost zones (<10 kg m^{-2}) to higher values in northly continuous and discontinuous permafrost zones (generally 10-25 kg m^{-2}) [*G Hugelius et al.*, 2013b]. Surficial rock OC follows a similar spatial pattern, which may be linked (even though rock was excluded from our permafrost estimates), with higher OC contents for sedimentary rock outcrops in northern Greenland (Figure S7). Greenland lakes display OC stocks which are orders of magnitude smaller than other land fringe components (4.1×10^{-4} to 3.6×10^{-2} PgC OC and 6.0×10^{-4} to 6.6×10^{-2} PgC IC), but are regionally important since they are hot spots for biological productivity [*N J Anderson et al.*, 2019].

3.2.4 Fjords and oceans Greenland fjords host OC and IC stocks which are orders of magnitude smaller than other components of our assessment (Figure 2, Dataset S1), but are important because of their links to productive fjord foodwebs and carbon burial [*L Meire et al.*, 2017; *R W Smith et al.*, 2015]. Fjord benthic OC stocks (median=0.38 PgC) are similar to those in Greenland oceans when normalised by area (Figure S19), but fjord PIC stocks (median= 0.10 PgC) are lower, likely due to dilution of pelagic carbonate by terrestrial material, and high carbonate dissolution rates associated with OC degradation [*C Kierdorf*, 2006]. Thus, pelagic DIC (median=0.33 PgC) dominates the total fjord IC stock, while benthic OC stocks exceed those for pelagic DOC (median=0.01 PgC).

Northern polar ocean IC stocks account for 76% of the total Greenland IC reservoir, and as for fjords, host higher contributions of DIC compared to benthic PIC (DIC median =104 PgC, PIC median =13.2 PgC). OC stocks are an order of magnitude smaller at 23 PgC POC (median) and 2.9 PgC DOC (median), and thus marine OC comprises just 22-33% of total Greenland OC stocks. Greenland benthic POC stocks are significant compared with those reported for Arctic shelf seas (82.3 PgC POC, which excluded most of the Greenland shelf area [*J E Vonk et al.*, 2025]) and DOC concentrations in Greenland oceans are often higher than those in Antarctica (Figures S16 and S17), consistent with more productive waters in Greenland coastal regions which comprise a greater fraction of the ocean area here compared to Antarctica. Thus, total Greenland ocean POC and DOC stocks are 8 times and 30 times smaller respectively than those in Antarctica, compared to ocean areas and volumes which are 13 and 45 times smaller respectively. Overall, oceans around Greenland host: 1% and 0.3% of global ocean benthic POC [*T B Atwood et al.*, 2020] and PIC [*R E Zeebe*, 2012] respectively; around 0.4% of DOC [*D A Hansell*, 2013]; and 0.3% of DIC [*L Keppler et al.*, 2020] for a contribution to global ocean area and volume of 1% and 0.3% respectively [*B W Eakins and G F Sharman*, 2010]. This

signifies their similar importance as OC and DIC stores compared with other major world ocean basins, but with lower PIC storage. We note that we do not consider sub-sea permafrost, which could be an important carbon store in the northern polar oceans [*P P Overduin et al.*, 2019].

4. Methane and Carbon dioxide fluxes in Greenland and Antarctica

Fluxes of CH_4 and CO_2 across Greenland and Antarctica's ice to ocean domain have historically been poorly constrained and have yet to be considered comparatively. In the following sections we discuss these fluxes, which are summarised in Dataset S2, Figures 4 and S12 (we note that Antarctic terrestrial CO_2 fluxes are not presented in Figure 4 but provided in Dataset S2).

4.1 Methane fluxes

We report relatively low fluxes of methane to the atmosphere from Greenland terrestrial areas and fjords (0.07-7.9 Tg CH_4, Figure 4). While permafrost and inland waters have been highlighted as important methane emitters in polar regions [*M A Kuhn et al.*, 2021; *J Ramage et al.*, 2024], the small land and fjord areas and carbon stocks (Figure 2) around Greenland (0.4 x 10^6 km^2) result in low emissions at present. Our land fringe methane fluxes include small emissions from onshore hydrocarbon seeps, at 0.001-0.03 Tg CH_4 a^{-1}, but with high uncertainty over the number of onshore seepage sites and only one point measurement of seep CH_4 emissions in Greenland (Figures 3 and 4). We note that our minimum flux estimate is of a similar order to fluxes recently calculated for Svalbard [*G E Kleber et al.*, 2023]. However, given the much higher area of Greenland land fringes (0.4 x 10^6 km^2) and limited surveys, true methane fluxes could be orders of magnitude higher than our assessment and require further scrutiny.

An intriguing aspect of our assessment is the potential flux of methane to the atmosphere from subglacial regions beneath the GrIS (Figure 4). We report a wide envelope of potential subglacial fluxes from 0.03 Tg CH_4 a^{-1} for 10 % of the ablation zone but up to 7.7 Tg CH_4 a^{-1} if methane is produced over the entire ablation zone at rates similar to glacier-fed ice-marginal lakes (Text S2, Figure 4). Our upper estimate is notable, given estimated total methane emissions of 9-53 Tg CH_4 a^{-1} from wetlands between 60 and 90 ºN [*M Saunois et al.*, 2020], 13.8-17.7 Tg CH_4 a^{-1} for high latitude lakes (>50 ºN) [*E Matthews et al.*, 2020], global median emissions of 55.8 Tg CH_4 a^{-1} for lakes and median emissions of 1.1 Tg CH_4 a^{-1} for rivers between 60 and 90 ºN [*J A Rosentreter et al.*, 2021]. However, we stress that these fluxes derive from upscaling from southwest Greenland and exclude factors that could amplify CH_4 fluxes, e.g. potential thermogenic sources in northeast Greenland, [*S Rysgaard et al.*, 2018]); and methane hydrate dissociation beneath inland ice, where methane is flushed by out by seasonal drainage development [*D M Chandler et al.*, 2013].

The source of subglacial methane has previously been inferred to be biological, generated by mixed sources (e.g. acetate fermentation and H_2/CO_2 [*M Dieser et al.*, 2014; *G Lamarche-Gagnon et al.*, 2019; *A J Pain et al.*, 2021]) or via H_2/CO_2 in basal material of the GRIP and GISP2 ice cores [*V Miteva et al.*, 2009; *R Souchez et al.*, 2006]. Its fast transport to the ice margin via efficient channels likely limits oxidative losses [*J R Christiansen and C J Jørgensen*, 2018; *G Lamarche-Gagnon et al.*, 2019]. The overlapping range of our rock OC and subglacial POC contents, and therefore, stock estimates (Section 3.2), imply that lithogenic

carbon may be a significant component of OC in inland subglacial regions, which adds further intrigue into how methane is generated beneath inland ice. One possibility is a mechanism which does not wholly rely on organic matter, for example, fuelled by hydrogen from rock comminution [*J Telling et al.*, 2015] and CO_2 from oxidative processes and/or atmospheric gas ingress to the subglacial drainage system. Another is that methane is generated in yet to be identified carbon-rich sedimentary basins or is associated with deep hydrocarbon seepage subglacially and released to the subglacial drainage system by diffusion and fluid flow. Methane fluxes from the AIS and its land fringes are still unknown due to a sparsity of data and require further study.

4.2 Carbon dioxide fluxes

Overall, Greenland land fringe and fjord sectors are either a small atmospheric sink or source for CO_2 (-15.5 to 8.7 TgC-CO_2 a^{-1}, Figure 4, Dataset S2), with negative fluxes from terrestrial permafrost, and positive fluxes from inland waters (rivers, lakes) and surficial rocks. The latter finding is broadly consistent with the entire Arctic [*J Ramage et al.*, 2024], however, significant bare rock areas in Greenland contribute further positive fluxes via the dominant effect of CO_2 from oxidative processes over CO_2 drawdown by silicate mineral weathering. We highlight uncertainty in Greenland land fringe CO_2 fluxes (-10.6 to 8 TgC-CO_2 a^{-1}) which reflects assumptions made about Greenland rivers: non-glacial Arctic rivers are net CO_2 emitters (1.9-3.9 TgC-CO_2 a^{-1}, Figure 4), while GrIS rivers represent a small short-term atmospheric CO_2 sink (-0.27 to -0.18 TgC-CO_2 a^{-1}, Figure 4). We expect that the latter is the most likely scenario for Greenland riverine CO_2 fluxes, arising from CO_2 under-saturation with respect to the atmosphere due to silicate and carbonate mineral dissolution in large ice sheet catchments (Text S2). Our Antarctic land fringe CO_2 fluxes only include rock weathering, which is a likely but highly uncertain source of CO_2 (0.27-17.5 TgC-CO_2 a^{-1}, Dataset S2). These derive from CO_2 released via sulphide oxidation/carbonate dissolution and OC oxidation that appear to exceed estimates of CO_2 drawdown by silicate mineral weathering, which matches assessments made across river catchments at lower latitudes where sedimentary rocks are present [*J R Zondervan et al.*, 2023].

Estimated atmospheric CO_2 fluxes associated with Greenland fjords indicate small negative to positive fluxes (-5.1 to 0.7 TgC-CO_2 a^{-1}). We expect the negative flux values are more likely, since a net annual drawdown of CO_2 is observed in all reported (n=3) glacially-fed Greenland fjords ([*L Meire et al.*, 2015; *S Ruiz-Halpern et al.*, 2010; *S Rysgaard et al.*, 2012]. The negative flux equates to 19-31% of total estimated CO_2 uptake in Greenland´s coastal ocean [*H C Henson et al.*, 2024] and is significant given the relatively small area (0.06 x 10^6 km^2) (Figure 2). Fjord CO_2 fluxes reflect a balance between processes which drive CO_2 undersaturation in surface waters (e.g. net ecosystem metabolism, de-nitrification, input of glacial meltwaters, surface cooling and anthropogenic emissions) and CO_2 saturation (e.g. aerobic degradation of riverine POC and DOC, nitrification, fjord hydrodynamics). Our PP estimates in Greenland fjords are -2.9 and -2.0 (range=-4.2 to -0.4) TgC a^{-1} via the ice-free period and MTG methods respectively (Section 2.5), where uncertainty associated with the MTG method underscores high inter-fjord variability and limited observations. In comparison, median land-fjord lateral fluxes of OC from Greenland are 0.19 TgC DOC and 2.3 TgC POC via rivers, and 1.1 TgC as POC+DOC via icebergs (Figure S12). These are of a similar order of magnitude to previous calculations [*E Hood et al.*, 2015], but highlight a significant POC flux of over a quarter of total

fluxes from Arctic rivers (8.2 TgC, [*J E Vonk et al.*, 2025]). An estimated vertical transport of -8.4 TgC a^{-1} OC from the upper mixed layer to the fjord benthos suggests a contribution from both autotrophically produced and laterally transported OC. The POC burial flux is -2.7 TgC a^{-1} (empirical estimate, Figure S12) to -0.5 TgC a^{-1} (modelled estimate over 1m), where the former is equivalent to 15% of global fjord POC burial and similar to previous global estimates scaled to Greenland fjord areas [*R W Smith et al.*, 2015].

Land-fringe and fjord carbon fluxes are dwarfed by air-sea exchange of CO_2 in the polar oceans (Figure 4). These are an important control on atmospheric CO_2 concentrations, influenced by a complex suite of physical, chemical and biological processes which play out differently across major ocean basins [*T H Peng and T Takahashi*, 1993]. In Antarctica, the Southern Ocean has long been highlighted as a major carbon sink, which reflects the exchange of natural CO_2, the uptake of anthropogenic CO_2, with additional climate-driven perturbations arising from changes in ocean circulation and biological productivity [*F Bunsen et al.*, 2024; *K Caldeira and P B Duffy*, 2000; *T L Frölicher et al.*, 2015; *N Gruber et al.*, 2019; *S E Mikaloff Fletcher et al.*, 2007]. The sub-tropical seasonally stratified biome (STSS), while outside of our study region, is the most significant Southern Ocean net CO_2 sink (-530 +/- 170 Tg C-CO_2 (via GBMs) and 620 +/- 50 Tg C-CO_2 (via pCO_2 products), largely due to sinking of waters at the Southern and Northern Tropical Fronts and cooling of southward moving water from the sub-tropics [*N Gruber et al.*, 2019; *J Hauck et al.*, 2023].

Observation-based pCO_2 product estimates of air-sea exchange fluxes of CO_2 from the ICE and SPSS biomes (mean and standard deviation) indicate modest fluxes into the ocean, but with high uncertainty, with -47 Tg C-CO_2 a^{-1} +/- 20 Tg C-CO_2 a^{-1} for the ICE Biome and -70 Tg C-CO_2 a^{-1} +/- 20 Tg C-CO_2 a^{-1} for the SPSS biome. GOBMs report slightly larger fluxes into the ocean, but a larger ensemble spread, at -86 +/- 126 Tg C-CO_2 a^{-1} (ICE) and -126 +/- 141 Tg C-CO_2 a^{-1} (SPSS). These net CO_2 fluxes are smaller than those reported for the STSS biome, and largely reflect the balance of outgassing of natural CO_2 and uptake of anthropogenic CO_2. Outgassing of natural CO_2 occurs in both the ICE and SPSS biomes due to upwelling of deep waters rich in natural CO_2, particularly during winter. However, fluxes of CO_2 outgassing are partially suppressed by rising atmospheric CO_2 from anthropogenic sources, which drives stronger ocean CO_2 uptake and thus increases the pCO_2 in surface ocean waters, particularly in the SPSS [*J Hauck et al.*, 2023]. This exceeds the opposing effect of climate-driven shifts in wind patterns, which strengthen upwelling and CO_2 outgassing in the SPSS [*J Hauck et al.*, 2023]. The large sea-ice extent in the ICE biome acts to reduce winter outgassing, and in spring and summer melting of the sea ice rapidly stratifies the water column, allowing biological productivity to draw down the CO_2 upwelled in the winter months [*D C E Bakker et al.*, 2008; *J Hauck et al.*, 2023].

We report modest uptake of CO_2 in Greenland oceans across both observation-based pCO_2 products (-81 +/-19 Tg C-CO_2 a-1) and GOBMs (-80 +/-31 Tg C-CO_2 a^{-1}), with 60% of the fluxes from south Greenland <65°N (Section 3.2.3, Figures S14 and S17). Our assessment compares with previous estimates for shelf areas of the northern/southern Greenland and Labrador Seas (-35.3 Tg C-CO_2 a^{-}1 [*G G Laruelle et al.*, 2014]). However, it spans a larger area, including the North Atlantic, which is a well-known global hot spot for CO_2 uptake due to deep water formation, high seasonal winds over low pCO_2 waters and enhanced primary productivity [*C T A Chen et al.*, 2013; *J Olafsson et al.*, 2021; *F F Pérez et al.*, 2024; *T Takahashi et al.*, 2002;

T Takahashi et al., 2009]. Air-sea exchange fluxes of CO_2 for Greenland´s oceans are 1.5-2.5 times smaller than the Southern Ocean, over a 13 times smaller area (Figures 1 and 4), and contribute by 4% to global ocean CO_2 fluxes for just 1% of ocean area [*P Friedlingstein et al.*, 2021]. However, we note that this is partly a product of the areas selected and the greater dominance of coastal areas versus open ocean in Greenland versus Antarctica. The role of biological productivity in contributing to elevated Greenland fluxes (by area) is consistent with our OC store assessment, which indicates higher marine POC/DOC stocks than in Antarctica when normalised by area/volume (Dataset S2).

Overall, our data indicate that the Greenlandic region likely has small positive fluxes of methane (0.1-7.9 Tg a^{-1} CH_4 or 1.6-172 and 0.5-58 TgC CO_2-equivalent a^{-1} using Global Warming Potentials of 20 years and 100 years respectively, *[P Forster et al., 2021]* Dataset S2), with the largest potential source from the GrIS. This equates to roughly 0.01-1% of global emissions (bottom-up estimates, 737 Tg CH_4 a^{-1} [*M Saunois et al.*, 2020]) and up to 20% of net methane fluxes from the entire Arctic permafrost region [*J Ramage et al.*, 2024]. The Greenlandic region represents a sink for CO_2 (-40 to -126 TgC-CO_2), dominated by the oceans (Dataset S2). In Antarctica, there is high uncertainty, but the entire region is most likely to be a modest sink for atmospheric CO_2 driven by the oceans (Dataset S2). However, data limitations prevent quantification of methane fluxes. While these flux estimates are useful, they are associated with high uncertainty (Figure 3) which is important to narrow given the sensitivity of this region to change under polar warming scenarios (Section 5).

5. Future change and opportunities for research

Ice Sheets and their surrounding marine and terrestrial environments are highly climatically sensitive and connected by flows of water, sediments and associated chemical loads which are active over diverse spatial and temporal scales. Unravelling the future climate impacts on carbon cycles at both poles must, therefore, consider multiple components of ice-land-ocean-atmosphere systems simultaneously and in an integrated manner. Both carbon stores and GHG fluxes across our polar domain are associated with order of magnitude uncertainty (Figure 3 and 5), and many carbon stocks and flux terms are unknown (Figure 5). The high uncertainty, even at the present day, challenges a robust assessment of the future trajectories of carbon stores and emissions across our polar domain, and demands a vast improvement in data availability and model capability. Here we summarise some of the important considerations when assessing future change, and highlight scientific breakthroughs required to reduce current uncertainties.

There has been radical shift in our view of ice sheets as “zero GHG flux zones” over the past two decades. The potential for ice sheets to cap substantial hydrocarbon reserves, including methane hydrate [*J L Wadham et al.*, 2012] is particularly relevant when considering projected ice sheet mass loss. Glaciated settings are predisposed to focussed release of such geologic carbon due to enhanced erosion of cap rocks, promoting seal breaching, along with repeated ice loading and unloading which encourages pressurisation of reservoirs and fluid migration via fault reactivation [*K Andreassen et al.*, 2017; *P Serov et al.*, 2017; *K M Walter Anthony et al.*, 2012]. An increasing number of studies report methane emissions via seeps and groundwater springs both in the southern [*A R Thurber et al.*, 2020] and northern hemispheres [*G E Kleber et al.*, 2023; *G E Kleber*

et al., 2024; *K M Walter Anthony et al.*, 2012]. This has been linked to glacier retreat, postulated to drive unloading of deep subglacial carbon reserves, permafrost degradation at glacier margins and formation of new proglacial land and shallow sub-sea surfaces, which activate focussed fluid flow between the subglacial and proglacial or coastal environments, termed the ”cryospheric cap” hypothesis [*K M Walter Anthony et al.*, 2012]. These methane sources are not included in polar methane budgets, despite the sensitivity of sub-cap carbon stores to ice sheet change [*K Andreassen et al.*, 2017]. Unlike permafrost regions, there are currently no spatially discretised maps of carbon stores beneath ice sheets and fluxes of methane to the atmosphere can only be crudely inferred from a few sites, challenging upscaling. Narrowed uncertainty of carbon stores and fluxes requires ice-sheet wide internationally-coordinated sampling missions, deep-drilling to representative sedimentary basins, and extensive geophysical studies. It also requires significant improvement in coupled physical-biogeochemical numerical models which can be applied at ice sheet scales and validated in representative ice sheet-carbon systems.

While our land fringe carbon stock and GHG flux estimates were relatively small (Figure 5), they are sensitive to future change via increases in net ecosystem production and above ground biomass in a warming climate [*M J Amesbury et al.*, 2017; *T A Day et al.*, 2008], along with increased glacial meltwater discharge and ice-marginal lake formation [*P How et al.*, 2021; *G Lamarche-Gagnon et al.*, 2019; *V Masson-Delmotte et al.*, 2012]. In addition, deglaciation, warming and permafrost thaw may also expose sulphide minerals and rock OC [*J T Crawford et al.*, 2019; *E V Walsh et al.*, 2024; *S Zolkos et al.*, 2018] with higher weathering rates [*G Soulet et al.*, 2021]. Our study highlights a need for better representation of land fringes in regional polar carbon assessments, including direct measurements of carbon stocks and fluxes, updated soil taxonomy to better accommodate Antarctic and Greenlandic soils and consideration of glacially-sourced rivers and newly-formed proglacial lakes as chemically distinct systems compared to non-glaciated regions of the Arctic.

Greenland fjords can be associated with strong CO_2 sinks (by area), despite the relatively small carbon pool and have relevance for regional carbon cycles [*R W Smith et al.*, 2015] and coastal ecosystem productivity [*M J Hopwood et al.*, 2020]. Given the importance of fjord primary and export production in supporting fjord foodwebs and the viability of fisheries in Greenland [*L Meire et al.*, 2017], narrowing uncertainty is a priority and requires a wider array of local-based assessments across fjord systems with differing glacial influences and across all sectors of Greenland, alongside numerical models with strong process representation which allow future trajectories of fjord productivity and carbon export to be predicted.

Marine carbon stores are sensitive to future changes in ocean productivity, circulation and chemistry, where shifts in the polar cryosphere are an important contributor [*S L Deppeler and A T Davidson*, 2017; *S F Henley et al.*, 2020; *G G Laruelle et al.*, 2014; *M H Pinkerton et al.*, 2021]. However, predicting the future of carbon cycling in the polar oceans is fraught with uncertainty. For example, a multitude of confounding factors have the potential to shift air-sea CO_2 exchange in different directions, which influence marine DIC and DOC pools, and play out against a backdrop of changing CO_2 uptake linked to anthropogenic emissions [*J Hauck et al.*, 2023; *J Hauck et al.*, 2015; *P Mongwe et al.*, 2024].

Sea ice reduction has important physical effects; in Arctic shelf seas it may increase air-sea exchange of CO_2 and strengthen uptake by increasing ocean surface area [*G G Laruelle et al.*, 2014; *S Yasunaka et al.*,

2023], but in the Southern Ocean it is likely to drive enhanced CO_2 outgassing in coastal regions [*E H Shadwick et al.*, 2021] which may only be partially compensated by increased biological productivity [*M Gupta et al.*, 2020; *J Hauck et al.*, 2015]. In the latter case, removal of the sea-ice lid impacts nutrient and light availability, strengthening the biological carbon pump by stimulating plankton productivity [*S L Deppeler and A T Davidson*, 2017; *S F Henley et al.*, 2020; *E F Møller et al.*, 2022]. Under future high emissions scenarios, polar regions of the Southern Ocean may shift towards greater CO_2 uptake as sea-ice melt freshens and stratifies the upper ocean, reducing winter outgassing and favouring solubility-driven CO_2 uptake [*P Mongwe et al.*, 2024].

However, the impact of ice sheets is in general understudied in most pan-polar assessments of ocean CO_2 exchange. The input of cold freshwaters from ice sheets (and sea ice) has additional contrasting impacts, for example, by enhancing CO_2 uptake in some coastal regions due to changes in CO_2 saturation [*S Rysgaard et al.*, 2009], but reducing CO_2 sequestration by dampening deep convection which influences the formation of Atlantic Deep Water [*C W Böning et al.*, 2016; *A Bretones et al.*, 2022; *Q Yang et al.*, 2016] and Antarctic Bottom Water [*C Nissen et al.*, 2022]. Direct and indirect glacial meltwater fertilisation of oceans may also drive CO_2 uptake via increased biological productivity, as indicated by past observational studies in Greenland [*K R Arrigo et al.*, 2017; *M Oksman et al.*, 2022; *H Oliver et al.*, 2018; *K Perner et al.*, 2019] and the Southern Ocean [*A C Alderkamp et al.*, 2012; *K R Arrigo et al.*, 2015; *L J A Gerringa et al.*, 2012]. However, model studies generate order of magnitude differences in glacier fertilisation-driven biological CO_2 uptake in Antarctica [*R Death et al.*, 2014; *C Lancelot et al.*, 2009; *C Laufkötter et al.*, 2018; *R Person et al.*, 2019]. Constraining the present and future impacts of cryospheric change on ocean CO_2 fluxes requires a better understanding of these complex ice-ocean feedbacks via observations, modelling (e.g. Earth System Models which include interactive ice sheets, [*P Mongwe et al.*, 2024]), remote sensing and palaeo-oceanographic study.

6. Conclusions

Overall, our assessment signifies that ice sheets and their surrounding terrestrial and marine environments are large carbon stores, hosting around 5300-22,200 PgC of organic carbon and 5600-8600 PgC of inorganic carbon (Figure 5). However, carbon stores and fluxes across our polar domains have order of magnitude uncertainty, which reflects sparse data and challenges of remote sensing and modelling in areas which are remote and perennially or seasonally ice-covered. Both of our polar domains are most likely to be overall sinks for GHGs, although there is high uncertainty (-125 to 18 and -480 to 72 TgC a^{-1} CO_2-equivalent a^{-1} for Greenland and Antarctica respectively, assuming Global Warming Potentials of 100 years for CH_4, Figure 5), but assessing the future trajectory of GHG fluxes within this complex multi-dimensional ice-to-ocean domain is impossible with the currently available data. We highlight several important areas for future study. First, are the carbon stores and fluxes associated with the polar ice sheets, and particularly subglacial CH_4 fluxes and the potential for methane hydrate storage at ice sheet beds, which has the potential to be destabilised by ice thinning. Second, are carbon stores and fluxes within land-fringes and fjords, which have regional importance since they support productive polar ecosystems and their services and exhibit sensitivity to climate warming. Third, are the very large carbon stores associated with polar oceans, which are substantial sinks for CO_2 though

with large associated uncertainty. Delimiting the present and future roles of physical/dynamical ocean change and that of the biological carbon pump on air-sea CO_2 exchange are critical to resolve and require integrated modelling-observational study. Dramatic changes are projected across this region, due to polar ice cap shrinkage, reduced sea ice and physical and biogeochemical changes in land fringes, fjords and oceans. This makes resolving current uncertainties vital to predict ice sheet-carbon cycle feedbacks in the 21st century and beyond.

Acknowledgements

We acknowledge the support of the Global Carbon Project's second REgional Carbon Cycle Assessment and Processes study (RECCAP2), and support from A. Bastos and P. Canadell. This research was a part of the Centre for Arctic Gas Hydrate, Environment, and Climate (CAGE) and the Centre for ice Cryosphere, Carbon and Climate (iC3) and was supported by the Research Council of Norway through its Centre of Excellence funding scheme (grants 223259 and 332635 respectively). We acknowledge the following funding sources: Royal Society Wolfson Merit Award to Wadham, The European Union´s Horizon 2020 Research and Innovation Programme under grant agreements 773421 and 101133587 to Hugelius and Ramage and the Swedish Academy of Science (Formas) under grant number FR-2021/0004 to Ramage. Laruelle is a research associate of the FRS-FNRS at the Université Libre de Bruxelles. Judith Rosentreter was funded through the funded through an ARC DECRA Fellowship (DE240100305). Hauck received funding from the Initiative and Networking Fund of the Helmholtz Association (Helmholtz Young Investigator Group Marine Carbon and Ecosystem Feedbacks in the Earth System [MarESys], grant number VH-NG-1301) and from the European Research Council (ERC-2022-STG OceanPeak, grant 101077209). Views and opinions expressed are however those of the author(s) and do not necessarily reflect those of the European Union or European Research Executive Agency. Neither the European Union nor the granting authority can be held responsible for them. Gregor was funded by the European Union's Horizon 2020 research and innovation programme under Grant 820989 (project COMFORT). Hilton and Zondervan were funded by the ERC Starting Grant ROC-CO_2 (project #678779 to Hilton). Hendry was supported by the BIOPOLE National Capability Multicentre Round 2 funding from the Natural Environment Research Council (grant no. NE/W004933/1). We thank Dr Mariana Esteves for her help with the drafting of figures for this manuscript.

Conflict of interest statement

The authors have no conflicts of interest to disclose.

Data Availability Statement

All stock and flux data reported in this paper are available in Supporting Information_ds01 and Supporting Information_ds02 respectively. GrIS runoff chemistry can be found at https://zenodo.org/records/7410609 and https://zenodo.org/records/7382723 [*G Lamarche-Gagnon et al.*, 2022a; *G Lamarche-Gagnon et al.*, 2022b]. Data used to calculate proglacial lake areas and volumes can be found at https://zenodo.org/records/7473753 [*J R Hawkings and S B Garcia-Yoa*, 2022]. DIC and pCO_2 data used to estimate glacial riverine CO_2 fluxes

can be found at https://zenodo.org/records/17660900 [*E Bagshaw et al.*, 2025]. All other data sources used to provide estimations are cited in the text and detailed in the Supporting Information.

Figure Captions

Figure 1 Regions considered in this RECCAP2 assessment for a. Greenland and b. Antarctica.

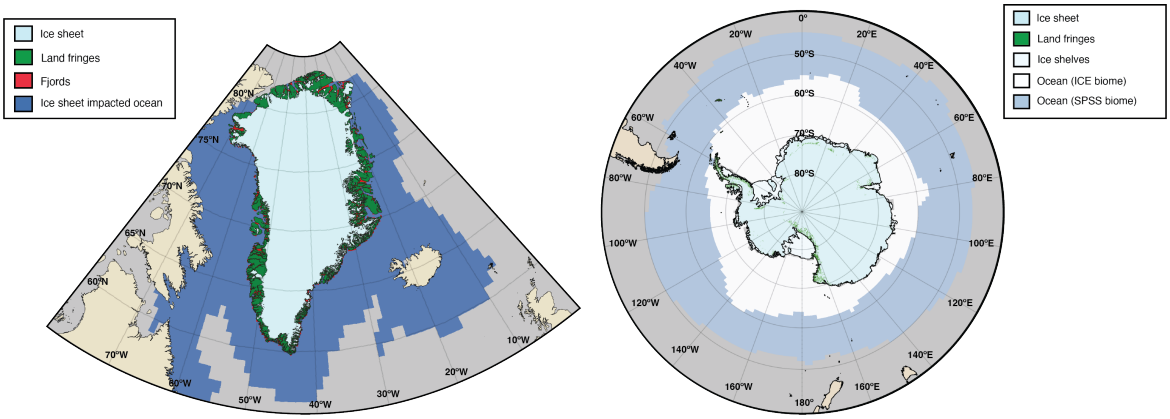

		Area (10^6 km^2)	Volume (10^6 km^3)
Greenland	Ice Sheet	1.70	2.9
	Land Fringes	0.41	-
	Fjords	0.06	0.01
	Oceans	3.66	3.92
	Deep hydrocarbons (oil and gas)	1.05[a]/3.24[b]	-
	All sectors (ex. hydrocarbons)[c]	5.83	
Antarctica	Ice Sheet	12.0	27.9
	Land Fringes (rock/permafrost)	1.48/0.03	-
	Southern Ocean (ICE)	18.7	63.3
	Southern Ocean (SPSS)	30.3	117.2
	Deep hydrocarbons (oil and gas)	8.91[d]/4.81[e]	-
	All sectors (ex. hydrocarbons[c]	62.5	-
TOTAL	All sectors (ex. hydrocarbons)[c]	68.3	-

a. Gautier et al (2009), b. From The Greenland Resource Assessment (2023).
c. Total areas exclude those for deep hydrocarbons due to overlapping areas with ice sheets.
d. From St John (1986) based on sedimentary basins over which oil and gas reserves were calculated, e. From Kingston (1992) based on geological provinces with oil and gas potential.

Figure 2a. Greenland organic (OC) and inorganic (IC) carbon stores for water column, glacial ice and shallow (<1m) sediments/rock/permafrost in ocean, land fringe, ice sheet, fjord and proglacial lake environments b. Antarctic OC and IC stores for water column, glacial ice and shallow (<1m) sediments/rock/permafrost in ocean (SPSS and ICE Biomes), land fringe and ice sheet environments, c. and d. Deep carbon stores in Greenland and Antarctica respectively, as deep hydrocarbons (oil and gas), marine/subglacial methane hydrate, and deep subglacial sediments (>1m). B_O/B_F = ocean/fjord benthic pools, P_O/P_F = ocean/fjord pelagic pools, PF=permafrost <1m, SR= surficial rocks <1m, $DC+PC_{ICE}$=dissolved + particulate carbon in glacial ice, PG= pelagic carbon pools in proglacial lakes, HC= deep hydrocarbons as oil and gas, M_O/M_{SG} = marine/subglacial methane hydrate, SG>1m = deep (>1m) subglacial sediments. Box plots = median, IQR, IQR+1.5x IQR, Points = mean/standard deviation, apart from PL (median, max and min) and HC, where we report data in previous studies (Dataset S1). Connected dashed points = maximum/ minimum, and violin plots represent model data [J L Wadham et al., 2012]).

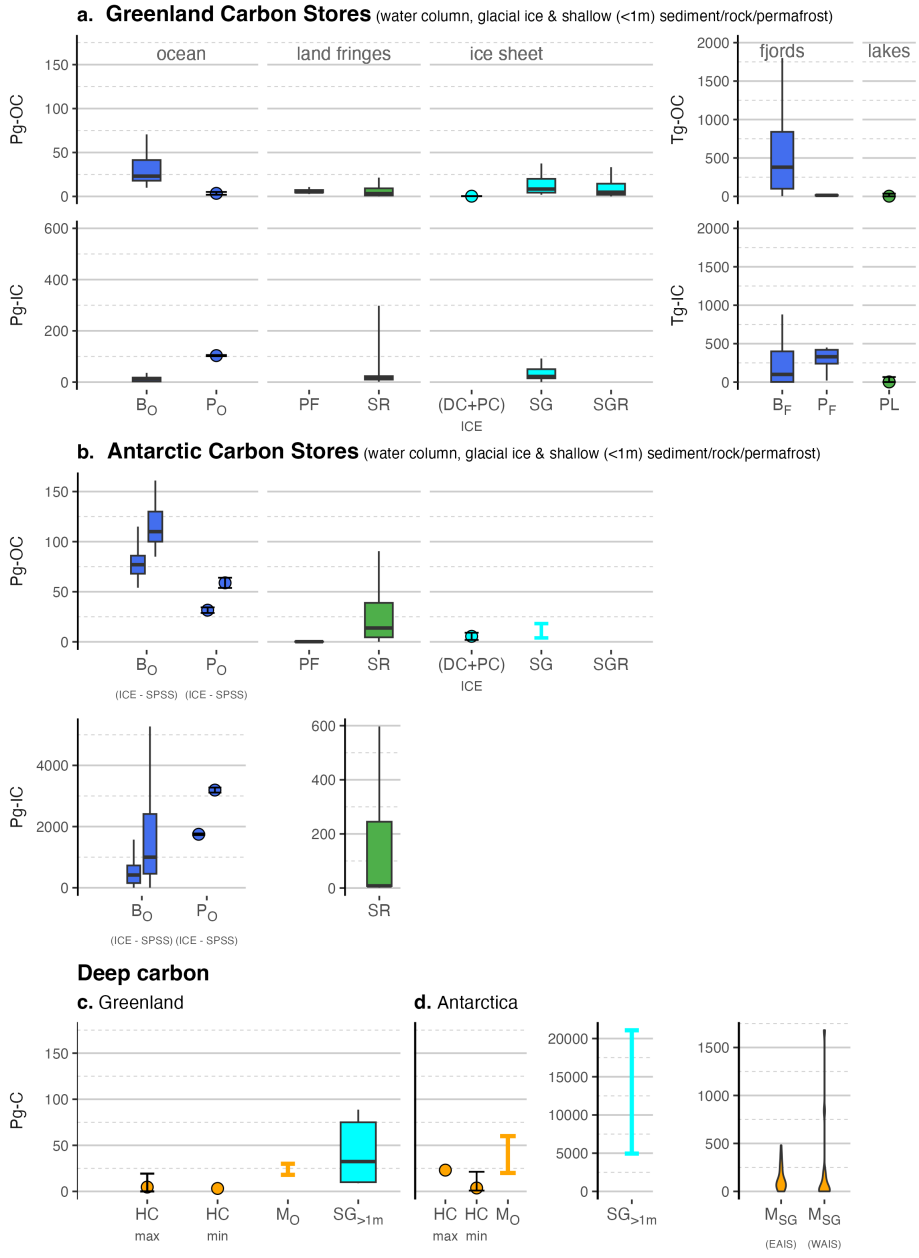

Figure 3 Summary of uncertainty and data gaps in polar carbon stores and fluxes (carbon stores include DOC/POC and DIC/PIC stocks listed in Table 1 for each sector of our polar domain, size= mid-range/median value, range= min/max and upper/lower respectively in Datasets S1 and S2. NB. for Land Fringes, the permafrost OC stock employs $OC_{PF<3m}$ and the GrIS OC stock uses $OC_{SG<1m}$+ $OC_{SG>1m}$ but not OC_{SGR}. Positive fluxes of CO_2 and CH_4 = fluxes into the atmosphere and negative fluxes = fluxes out of the atmosphere).

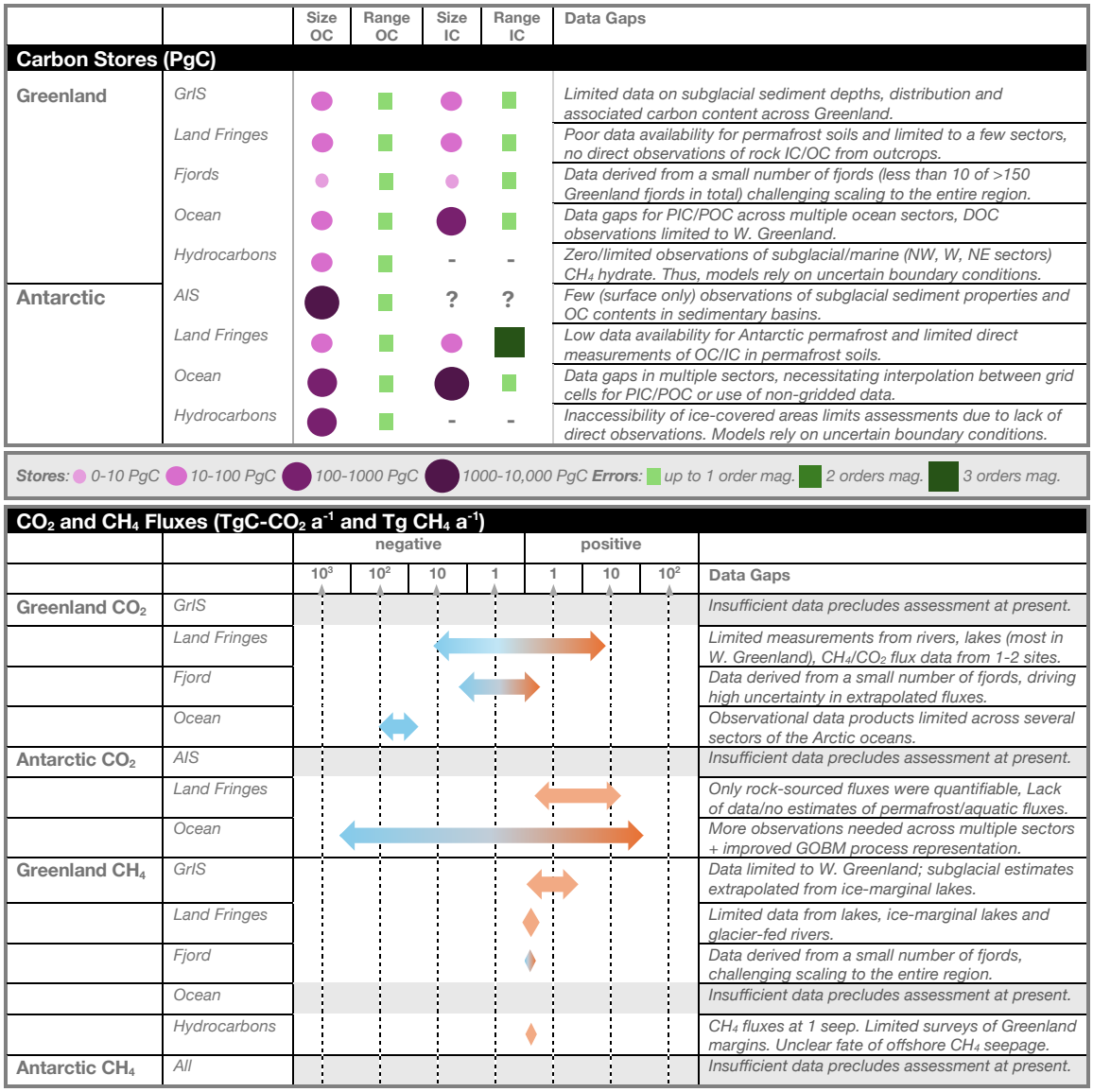

Figure 4 Fluxes of a. CO_2 and b. CH_4 from Greenland land fringes, the GrIS and fjords, c. CO_2 from Greenland oceans and d. CO_2 from the Southern Ocean using observation-based pCO_2 products and Global Biogeochemistry Models (GOBMs) (Petro-OC = petrogenic organic carbon oxidation, seeps = hydrocarbon seeps). In a./b., we report: the mean/95% confidence interval (permafrost and fjords); minimum/maximum estimates as bars (rock carbon and GrIS); a single estimate of CH_4 fluxes (seeps); Greenland-wide total CO_2 fluxes are calculated from summed non-ice sheet fluxes and assuming riverine fluxes similar to Arctic rivers (upper estimate from summed red bars) or similar to GrIS rivers (lower estimate). Total CH_4 fluxes include summation of GrIS (blue bars) and non-ice sheet CH_4 fluxes (red bars), with different assumptions around subglacial CH_4 emissions (10-100% of ablation zone) to generate lower/upper estimates. In b., we also report CH_4 fluxes as C-CO_2 equivalent a^{-1} for a GWP100 or GWP20 [P Forster et al., 2021]. The Southern Ocean refers to the Subpolar Seasonally Stratified (SPSS) and seasonally ice-covered (ICE) biomes and excludes the Subtropical Seasonally Stratified biome (STSS); with reported mean/standard deviation. See Dataset S2.

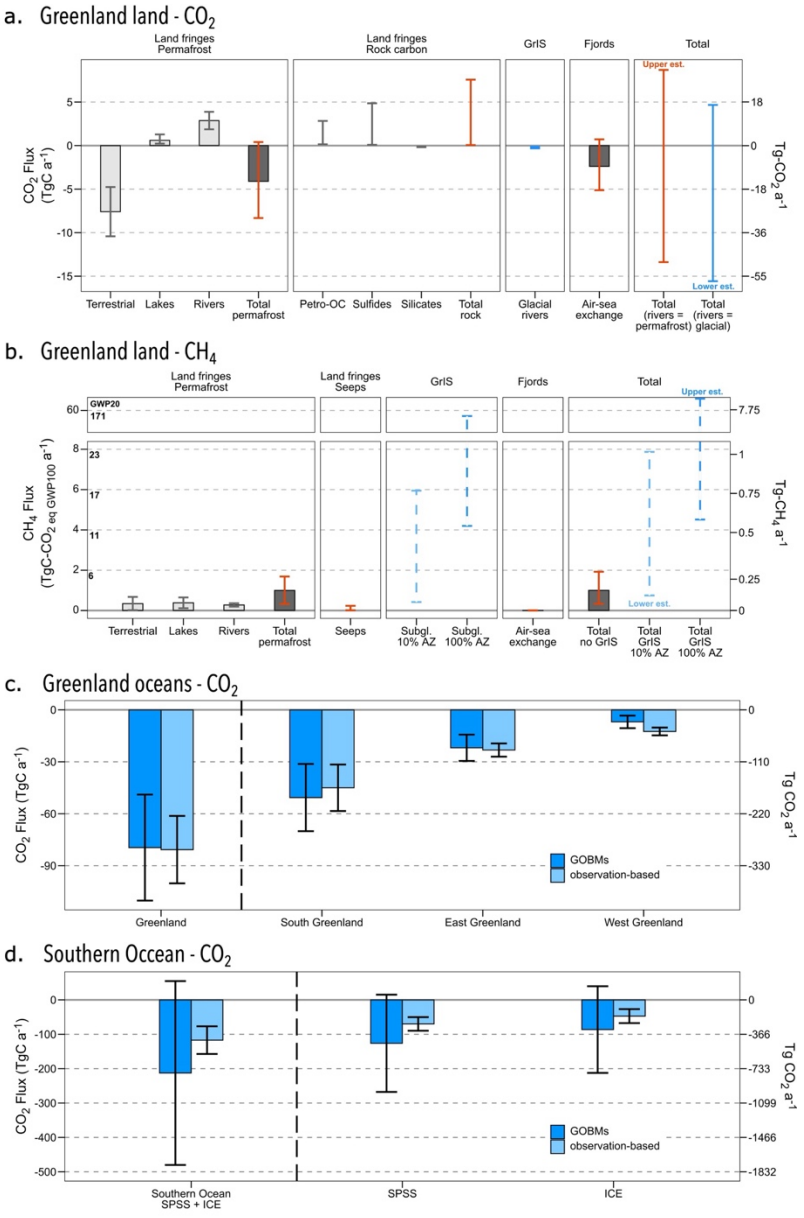

Figure 5 Conceptual diagram summarising carbon stocks (to 2 sig. figs. or 1-2 d.p.s) and atmospheric fluxes of CO_2 and CH_4 ($TgC\text{-}CO_2\ a^{-1}$and $Tg\ CH_4\ a^{-1}$) in a. Greenland and b. Antarctica. Stocks are in PgC, and we report the IQR or the full range. For oil and gas reserves, we report minimum and maximum estimates, and for Antarctic subglacial methane hydrate+free gas we report the most probable modelled range [J L Wadham et al., 2012]. For fluxes, we report lower and upper estimates or a single estimate if a range is unavailable (see Supporting Information, Introduction). Net fluxes to the atmosphere are in $TgC\text{-}CO_2$ equivalent a^{-1} for (GWP100 and GWP20). We include estimates of Greenland fjord PP ("ice-free period" and "MTG" methods), and single value estimates of Greenland fjord POC burial and Greenland/Antarctic freshwater DOC/POC export via rivers and icebergs (in $Tg\ C\ a^{-1}$).

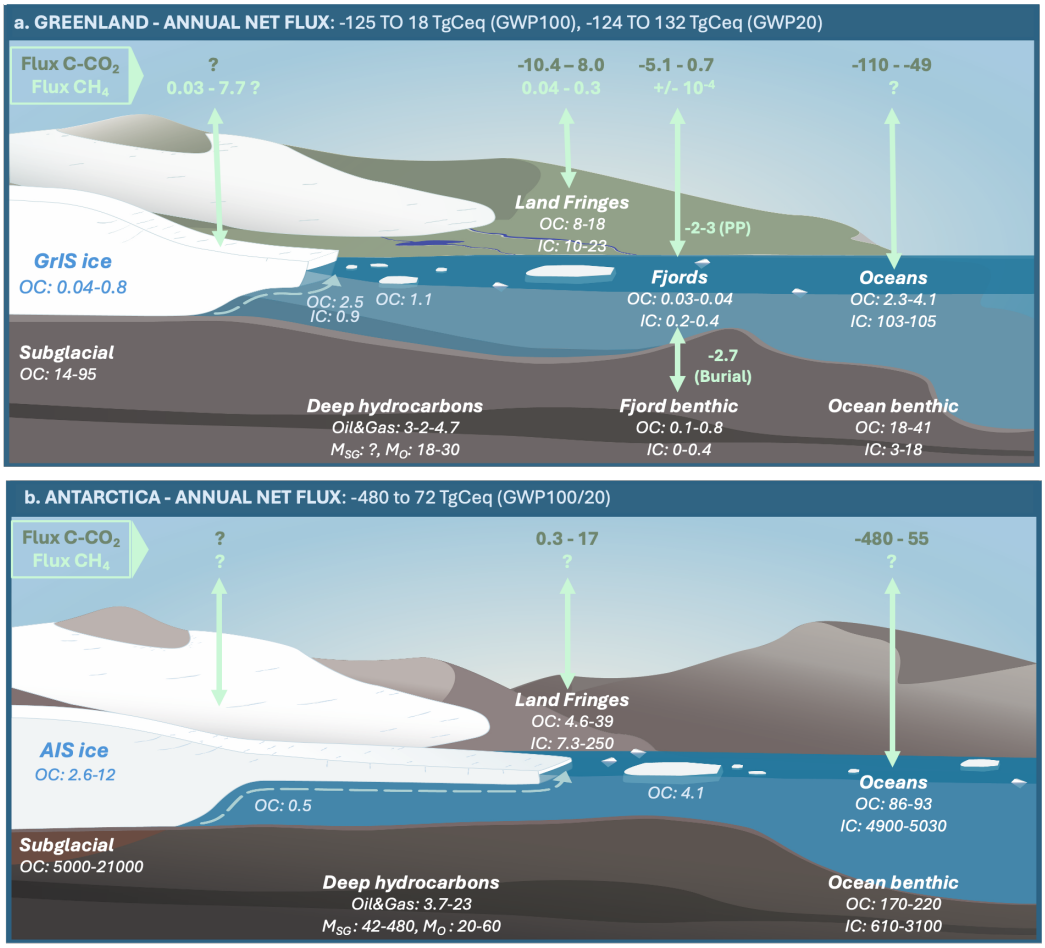

References:

Aitken, A. R., L. Li, B. Kulessa, D. M. Schroeder, T. A. Jordan, J. M. Whittaker, S. Anandakrishnan, D. A. Wiens, O. Eisen, and M. J. Siegert (2022), Antarctica's subglacial sedimentary basins and their influence on ice-sheet change, *Earth and Space Science Open Archive*, 72.

Alderkamp, A. C., et al. (2012), Iron from melting glaciers fuels phytoplankton blooms in the Amundsen Sea (Southern Ocean): Phytoplankton characteristics and productivity, *Deep-Sea Res Pt Ii*, *71-76*, 32-48.

AMAP (2021), Arctic Climate Change Update 2021: Key Trends and Impacts. Summary for Policy-makers. Arctic Monitoring and Assessment Programme (AMAP)*Rep.*, AMAP, Tromsø, Norway.

Amesbury, M. J., T. P. Roland, J. Royles, D. A. Hodgson, P. Convey, H. Griffiths, and D. J. Charman (2017), Widespread Biological Response to Rapid Warming on the Antarctic Peninsula, *Current Biology*, *27*(11), 1616-1622.e1612.

Amiotte Suchet, P., J.-L. Probst, and W. Ludwig (2003), Worldwide distribution of continental rock lithology: Implications for the atmospheric/soil CO2 uptake by continental weathering and alkalinity river transport to the oceans, *Global Biogeochem Cy*, *17*(2).

Anderson, N. J., P. G. Appleby, R. Bindler, I. Renberg, D. J. Conley, S. C. Fritz, V. J. Jones, E. J. Whiteford, and H. Yang (2019), Landscape-Scale Variability of Organic Carbon Burial by SW Greenland Lakes, *Ecosystems*, *22*(8), 1706-1720.

Andreassen, K., et al. (2017), Massive blow-out craters formed by hydrate-controlled methane expulsion from the Arctic seafloor, *Science*, *356*(6341), Doi:10.1126/science.aal4500.

Andrews, M. G., A. D. Jacobson, M. R. Osburn, and T. M. Flynn (2018), Dissolved Carbon Dynamics in Meltwaters From the Russell Glacier, Greenland Ice Sheet, *Journal of Geophysical Research: Biogeosciences*, *123*(9), 2922-2940.

Anesio, A. M., and J. Laybourn-Parry (2012), Glaciers and ice sheets as a biome, *Trends Ecol Evol*, *27*(4), 219-225.

Arrigo, K. R., G. L. Van Dijken, and A. L. Strong (2015), Environmental controls of marine productivity hot spots around Antarctica, *Journal of Geophysical Research: Oceans*, *120*(8), 5545–5565.

Arrigo, K. R., G. L. van Dijken, R. M. Castelao, H. Luo, Å. K. Rennermalm, M. Tedesco, T. L. Mote, H. Oliver, and P. L. Yager (2017), Melting glaciers stimulate large summer phytoplankton blooms in southwest Greenland waters, *Geophys Res Lett*, Doi:10.1002/2017GL073583.

Atwood, T. B., A. Witt, J. Mayorga, E. Hammill, and E. Sala (2020), Global Patterns in Marine Sediment Carbon Stocks, *Frontiers in Marine Science*, *7*(165).

Bagshaw, E., G. Lamarche-Gagnon, J. Hawkings, P. Renforth, J. Hatton, A. Beaton, J. Telling, and J. L. Wadham (2025), Carbonate species from the Leverett and Kiatuut Sermia glacial rivers, Southwest Greenland, 2012-2015, edited, Zenodo, Global Biogeochemical Cycles.

Bagshaw, E. A., J. L. Wadham, M. Tranter, A. D. Beaton, J. R. Hawkings, G. Lamarche-Gagnon, and M. C. Mowlem (2021), Measuring pH in low ionic strength glacial meltwaters using ion selective field effect transistor (ISFET) technology, *Limnology and Oceanography: Methods*, *19*(3), 222-233.

Bakker, D. C. E., M. Hoppema, M. Schröder, W. Geibert, and H. J. W. de Baar (2008), A rapid transition from ice covered CO₂–rich waters to a biologically mediated CO₂ sink in the eastern Weddell Gyre, *Biogeosciences*, *5*(5), 1373-1386.

Balch, W. M., D. T. Drapeau, B. C. Bowler, E. Lyczskowski, E. S. Booth, and D. Alley (2011), The contribution of coccolithophores to the optical and inorganic carbon budgets during the Southern Ocean Gas Exchange Experiment: New evidence in support of the "Great Calcite Belt" hypothesis, *Journal of Geophysical Research: Oceans*, *116*(C4).

Bamber, J., A. Tedstone, M. King, I. Howat, E. Enderlin, M. van den Broeke, and B. Noel (2018), Modelled and observational freshwater flux time series for land ice in the Arctic and North Atlantic for 1958-2016 b, edited, British Oceanographic Data Centre, Natural Environment Research Council.

Baranov, A., A. Morelli, and A. Chuvaev (2021), ANTASed - An Updated Sediment Model for Antarctica, *Frontiers in Earth Science*, *9*.

Barnes, D. K. A., A. Fleming, C. J. Sands, M. L. Quartino, and D. Deregibus (2018), Icebergs, sea ice, blue carbon and Antarctic climate feedbacks, *Philos Trans A Math Phys Eng Sci*, *376*(2122).

Bhatia, M. P., S. B. Das, L. Xu, M. A. Charette, J. L. Wadham, and E. B. Kujawinski (2013), Organic carbon export from the Greenland ice sheet, *Geochim Cosmochim Ac*, *109*, 329-344.

Bierman, P. R., L. B. Corbett, J. A. Graly, T. A. Neumann, A. Lini, B. T. Crosby, and D. H. Rood (2014), Preservation of a Preglacial Landscape Under the Center of the Greenland Ice Sheet, *Science*, *344*(6182), 402-405.

Bockheim, J., G. Vieira, M. Ramos, J. López-Martínez, E. Serrano, M. Guglielmin, K. Wilhelm, and A. Nieuwendam (2013), Climate warming and permafrost dynamics in the Antarctic Peninsula region, *Global and Planetary Change*, *100*, 215-223.

Bockheim, J. G., and N. W. Haus (2014), Distribution of Organic Carbon in the Soils of Antarctica, in *Soil Carbon. Progress in Soil Science*, edited by A. Hartemink and K. McSweeney, Springer International Publishing

Böning, C. W., E. Behrens, A. Biastoch, K. Getzlaff, and J. L. Bamber (2016), Emerging impact of Greenland meltwater on deepwater formation in the North Atlantic Ocean, *Nat Geosci*, *9*(7), 523-527.

Booth, A. D., P. Christoffersen, C. Schoonman, A. Clarke, B. Hubbard, R. Law, S. H. Doyle, T. R. Chudley, and A. Chalari (2020), Distributed Acoustic Sensing of Seismic Properties in a Borehole Drilled on a Fast-Flowing Greenlandic Outlet Glacier, *Geophys Res Lett*, *47*(13), e2020GL088148.

Bretones, A., K. H. Nisancioglu, M. F. Jensen, A. Brakstad, and S. Yang (2022), Transient Increase in Arctic Deep-Water Formation and Ocean Circulation under Sea Ice Retreat, *J Climate*, *35*(1), 109-124.

Brosius, L. S., K. M. Walter Anthony, T. V. Lowell, P. Anthony, J. P. Chanton, M. C. Jones, G. Grosse, and A. J. Breckenridge (2024), Methane emissions from proglacial lakes: A synthesis study directed toward Lake Agassiz, *Quaternary Sci Rev*, *344*, 108975.

Bunsen, F., C. Nissen, and J. Hauck (2024), The Impact of Recent Climate Change on the Global Ocean Carbon Sink, *Geophys Res Lett*, *51*(4), e2023GL107030.

Burton-Johnson, A., M. Black, P. T. Fretwell, and J. Kaluza-Gilbert (2016), An automated methodology for differentiating rock from snow, clouds and sea in Antarctica from Landsat 8 imagery: a new rock outcrop map and area estimation for the entire Antarctic continent, *The Cryosphere*, *10*(4), 1665-1677.

Caldeira, K., and P. B. Duffy (2000), The Role of the Southern Ocean in Uptake and Storage of Anthropogenic Carbon Dioxide, *Science*, *287*(5453), 620-622.

Cameron, K. A., M. Stibal, J. R. Hawkings, A. B. Mikkelsen, J. Telling, T. J. Kohler, E. Gözdereliler, J. D. Zarsky, J. L. Wadham, and C. S. Jacobsen (2017), Meltwater export of prokaryotic cells from the Greenland ice sheet, *Environ Microbiol*, *19*(2), 524-534.

Carroll, D., et al. (2022), Attribution of Space-Time Variability in Global-Ocean Dissolved Inorganic Carbon, *Global Biogeochem Cy*, *36*(3), e2021GB007162.

Chandler, D. M., et al. (2013), Evolution of the subglacial drainage system beneath the Greenland Ice Sheet revealed by tracers, *Nat Geosci*, *6*(3), 195-198.

Chase, Z., K. E. Kohfeld, and K. Matsumoto (2015), Controls on biogenic silica burial in the Southern Ocean, *Global Biogeochem Cy*, *29*(10), 1599-1616.

Chen, C. T. A., T. H. Huang, Y. C. Chen, Y. Bai, X. He, and Y. Kang (2013), Air–sea exchanges of CO₂ in the world's coastal seas, *Biogeosciences*, *10*(10), 6509-6544.

Chen, J.-J., et al. (2023), Reduced Deep Convection and Bottom Water Formation Due To Antarctic Meltwater in a Multi-Model Ensemble, *Geophys Res Lett*, *50*(24), e2023GL106492.

Christ, A. J., et al. (2021), A multimillion-year-old record of Greenland vegetation and glacial history preserved in sediment beneath 1.4 km of ice at Camp Century, *Proceedings of the National Academy of Sciences*, *118*(13), e2021442118.

Christiansen, F., and J. Bojesen-Koefoed (2021), Inventory of onshore petroleum seeps and stains in Greenland: a web-based GIS model*Rep.*, 47 pp.

Christiansen, F. G. (2021), Greenland petroleum exploration history: Rise and fall, learnings, and future perspectives, *Resources Policy*, *74*, 102425.

Christiansen, J. R., and C. J. Jørgensen (2018), First observation of direct methane emission to the atmosphere from the subglacial domain of the Greenland Ice Sheet, *Scientific Reports*, *8*(1), 16623.

Christianson, K., L. E. Peters, R. B. Alley, S. Anandakrishnan, R. W. Jacobel, K. L. Riverman, A. Muto, and B. A. Keisling (2014), Dilatant till facilitates ice-stream flow in northeast Greenland, *Earth Planet Sc Lett*, *401*, 57-69.

Christner, B. C., et al. (2014), A microbial ecosystem beneath the West Antarctic ice sheet, *Nature*, *512*(7514), 310-313.

Colesie, C., M. Gommeaux, T. G. A. Green, and B. Büdel (2014), Biological soil crusts in continental Antarctica: Garwood Valley, southern Victoria Land, and Diamond Hill, Darwin Mountains region, *Antarct Sci*, *26*(2), 115-123.

Colgan, W., J. A. MacGregor, K. D. Mankoff, R. Haagenson, H. Rajaram, Y. M. Martos, M. Morlighem, M. A. Fahnestock, and K. K. Kjeldsen (2021), Topographic Correction of Geothermal Heat Flux in Greenland and Antarctica, *Journal of Geophysical Research: Earth Surface*, *126*(2), e2020JF005598.

Cook, A. J., P. R. Holland, M. P. Meredith, T. Murray, A. Luckman, and D. G. Vaughan (2016), Ocean forcing of glacier retreat in the western Antarctic Peninsula, *Science*, *353*(6296), Doi:10.1126/science.aae0017.

Cowton, T., P. Nienow, I. Bartholomew, A. Sole, and D. Mair (2012), Rapid erosion beneath the Greenland ice sheet, *Geology*, *40*(4), 343-346.

Cox, D. R., M. Huuse, A. M. W. Newton, P. Gannon, and J. Clayburn (2020), Slip sliding away: Enigma of large sandy blocks within a gas-bearing mass transport deposit, offshore northwestern Greenland, *AAPG Bulletin*, *104*(5), 1011-1043.

Cox, D. R., M. Huuse, A. M. W. Newton, A. D. Sarkar, and P. C. Knutz (2021), Shallow gas and gas hydrate occurrences on the northwest Greenland shelf margin, *Marine Geology*, *432*, 106382.

Crawford, J. T., E.-L. S. Hinckley, M. I. Litaor, J. Brahney, and J. C. Neff (2019), Evidence for accelerated weathering and sulfate export in high alpine environments, *Environ Res Lett*, *14*(12), 124092.

Csank, A. Z., C. I. Czimczik, X. Xu, and J. M. Welker (2019), Seasonal Patterns of Riverine Carbon Sources and Export in NW Greenland, *Journal of Geophysical Research: Biogeosciences*, *124*(4), 840-856.

Davis, C. L., et al. (2023), Biogeochemical and historical drivers of microbial community composition and structure in sediments from Mercer Subglacial Lake, West Antarctica, *ISME Commun*, *3*(1), 8.

Davison, B. J., A. J. Sole, S. J. Livingstone, T. R. Cowton, and P. W. Nienow (2019), The Influence of Hydrology on the Dynamics of Land-Terminating Sectors of the Greenland Ice Sheet, *Frontiers in Earth Science*, *7*(10).

Day, T. A., C. T. Ruhland, and F. S. Xiong (2008), Warming increases aboveground plant biomass and C stocks in vascular-plant-dominated Antarctic tundra, *Global Change Biology*, *14*(8), 1827-1843.

Death, R., J. L. Wadham, F. Monteiro, A. M. Le Brocq, M. Tranter, A. Ridgwell, S. Dutkiewicz, and R. Raiswell (2014), Antarctic ice sheet fertilises the Southern Ocean, *Biogeosciences*, *11*(10), 2635-2643.

DeFoor, W., M. Person, H. C. Larsen, D. Lizarralde, D. Cohen, and B. Dugan (2011), Ice sheet–derived submarine groundwater discharge on Greenland's continental shelf, *Water Resour Res*, *47*(7).

Deppeler, S. L., and A. T. Davidson (2017), Southern Ocean Phytoplankton in a Changing Climate, *Frontiers in Marine Science*, *4*, 40.

DeVries, T. (2022), The Ocean Carbon Cycle, *Annual Review of Environment and Resources*, *47*(Volume 47, 2022), 317-341.

Dickens, W. A., et al. (2019), Enhanced glacial discharge from the eastern Antarctic Peninsula since the 1700s associated with a positive Southern Annular Mode, *Scientific Reports*, *9*(1), 14606.

Dieser, M., E. L. J. E. Broemsen, K. A. Cameron, G. M. King, A. Achberger, K. Choquette, B. Hagedorn, R. Sletten, K. Junge, and B. C. Christner (2014), Molecular and biogeochemical evidence for methane cycling beneath the western margin of the Greenland Ice Sheet, *Isme J*, *8*(11), 2305-2316.

Dugan, H. A., P. T. Doran, D. Grombacher, E. Auken, T. Bording, N. Foged, N. Foley, J. Mikucki, R. A. Virginia, and S. Tulaczyk (2022), Brief communication: The hidden labyrinth: deep groundwater in Wright Valley, Antarctica, *The Cryosphere*, *16*(12), 4977-4983.

Eakins, B. W., and G. F. Sharman (2010), Volumes of the World's Oceans from ETOPO1, edited, p. 19, NOAA National Geophysical Data Center, Boulder, CO.

Etiope, G., G. Ciotoli, S. Schwietzke, and M. Schoell (2019), Gridded maps of geological methane emissions and their isotopic signature, *Earth Syst. Sci. Data*, *11*(1), 1-22.

Fay, A. R., and G. A. McKinley (2014), Global open-ocean biomes: mean and temporal variability, *Earth Syst. Sci. Data*, *6*(2), 273-284.

Forster, P., et al. (2021), The Earth's Energy Budget, Climate Feedbacks, and Climate Sensitivity, , in *Climate Change 2021: The Physical Science Basis.* , edited, pp. 923-1054, Cambridge University Press, Cambridge, United Kingdom and New York, USA.

Franke, S., D. Jansen, T. Binder, N. Dörr, V. Helm, J. Paden, D. Steinhage, and O. Eisen (2020), Bed topography and subglacial landforms in the onset region of the Northeast Greenland Ice Stream, *Annals of Glaciology*, *61*(81), 143-153.

Freitas, F. S., S. Arndt, K. R. Hendry, J. C. Faust, A. C. Tessin, and C. März (2022), Benthic Organic Matter Transformation Drives pH and Carbonate Chemistry in Arctic Marine Sediments, *Global Biogeochem Cy*, *36*(7), e2021GB007187.

Friedlingstein, P., et al. (2021), Global Carbon Budget 2021, *Earth Syst. Sci. Data Discuss.*, *2021*, 1-191.

Frölicher, T. L., J. L. Sarmiento, D. J. Paynter, J. P. Dunne, J. P. Krasting, and M. Winton (2015), Dominance of the Southern Ocean in Anthropogenic Carbon and Heat Uptake in CMIP5 Models, *J Climate*, *28*(2), 862-886.

Gautier, D. L., et al. (2009), Assessment of Undiscovered Oil and Gas in the Arctic, *Science*, *324*(5931), 1175-1179.

Gerringa, L. J. A., A. C. Alderkamp, P. Laan, C. E. Thuroczy, H. J. W. De Baar, M. M. Mills, G. L. van Dijken, H. van Haren, and K. R. Arrigo (2012), Iron from melting glaciers fuels the phytoplankton blooms in Amundsen Sea (Southern Ocean): Iron biogeochemistry, *Deep-Sea Res Pt Ii*, *71-76*, 16-31.

Gerrish, L., P. Fretwell, and P. Cooper (2020), High resolution Antarctic lakes dataset - VERSION 7.3, edited by N. E. R. C. Polar Data Centre, UK Research & Innovation.

Gill-Olivas, B., J. Telling, M. Tranter, M. Skidmore, B. Christner, S. O'Doherty, and J. Priscu (2021), Subglacial erosion has the potential to sustain microbial processes in Subglacial Lake Whillans, Antarctica, *Communications Earth & Environment*, *2*(1), 134.

Giustiniani, M., and U. Tinivella (2021), Gas Hydrates in Antarctica, in *Glaciers and the Polar Environment*, edited by M. Kanao, G. D. and N. Dematteis, pp. 1-19, IntechOpen CY, Rijeka.

Graly, J. A., L. B. Corbett, P. R. Bierman, A. Lini, and T. A. Neumann (2018), Meteoric 10Be as a tracer of subglacial processes and interglacial surface exposure in Greenland, *Quaternary Sci Rev*, *191*, 118-131.

Gregor, L., and N. Gruber (2021), OceanSODA-ETHZ: a global gridded data set of the surface ocean carbonate system for seasonal to decadal studies of ocean acidification, *Earth Syst. Sci. Data*, *13*(2), 777-808.

Gruber, N., P. Landschützer, and N. S. Lovenduski (2019), The Variable Southern Ocean Carbon Sink, *Annual Review of Marine Science*, *11*(1), 159-186.

Gupta, M., M. J. Follows, and J. M. Lauderdale (2020), The Effect of Antarctic Sea Ice on Southern Ocean Carbon Outgassing: Capping Versus Light Attenuation, *Global Biogeochem Cy*, *34*(8), e2019GB006489.

Gustafson, C. D., K. Key, M. R. Siegfried, J. P. Winberry, H. A. Fricker, R. A. Venturelli, and A. B. Michaud (2022), A dynamic saline groundwater system mapped beneath an Antarctic ice stream, *Science*, *376*(6593), 640-644.

Hansell, D. A. (2013), Recalcitrant Dissolved Organic Carbon Fractions, *Annual Review of Marine Science*, *5*(1), 421-445.

Hansell, D. A., and C. A. Carlson (1998), Deep-ocean gradients in the concentration of dissolved organic carbon, *Nature*, *395*(6699), 263-266.

Hansell, D. A., and M. V. Orellana (2021), Dissolved Organic Matter in the Global Ocean: A Primer, *Gels*, *7*(3).

Hartmann, J., and N. Moosdorf (2012), The new global lithological map database GLiM: A representation of rock properties at the Earth surface, *Geochemistry, Geophysics, Geosystems*, *13*(12).

Hauck, J., D. Gerdes, C.-D. Hillenbrand, M. Hoppema, G. Kuhn, G. Nehrke, C. Völker, and D. A. Wolf-Gladrow (2012), Distribution and mineralogy of carbonate sediments on Antarctic shelves, *J Marine Syst*, *90*(1), 77-87.

Hauck, J., et al. (2023), The Southern Ocean carbon cycle 1985-2018: mean, seasonal cycle, trends and storage, *Global Biogeochem. Cycles*, *37*.

Hauck, J., et al. (2015), On the Southern Ocean CO2 uptake and the role of the biological carbon pump in the 21st century, *Global Biogeochem Cy*, *29*(9), 1451-1470.

Hawkings, J. R., and S. B. Garcia-Yoa (2022), Greenland lake areas, volumes and depths, edited, Zenodo.

Hawkings, J. R., et al. (2021), Large subglacial source of mercury from the southwestern margin of the Greenland Ice Sheet, *Nat Geosci*.

Heathcote, A. J., P. A. del Giorgio, and Y. T. Prairie (2015), Predicting bathymetric features of lakes from the topography of their surrounding landscape, *Can J Fish Aquat Sci*, *72*(5), 643-650.

Henley, S. F., et al. (2020), Changing Biogeochemistry of the Southern Ocean and Its Ecosystem Implications, *Frontiers in Marine Science*, *7*.

Henson, H. C., M. Sejr, L. Meire, L. L. Sørensen, M. H. S. Winding, and J. M. Holding (2024), Resolving Heterogeneity in CO2 Uptake Potential in the Greenland Coastal Ocean, *Journal of Geophysical Research: Biogeosciences*, *129*(12), e2024JG008246.

Henson, H. C., J. M. Holding, L. Meire, S. Rysgaard, C. A. Stedmon, A. Stuart-Lee, J. Bendtsen, and M. Sejr (2023), Coastal freshening drives acidification state in Greenland fjords, *Sci Total Environ*, *855*, 158962.

Hilton, R. G., and A. J. West (2020), Mountains, erosion and the carbon cycle, *Nature Reviews Earth & Environment*, *1*(6), 284-299.

Hofstede, C., P. Christoffersen, B. Hubbard, S. H. Doyle, T. J. Young, A. Diez, O. Eisen, and A. Hubbard (2018), Physical Conditions of Fast Glacier Flow: 2. Variable Extent of Anisotropic Ice and Soft Basal Sediment From Seismic Reflection Data Acquired on Store Glacier, West Greenland, *Journal of Geophysical Research: Earth Surface*, *123*(2), 349-362.

Hood, E., T. J. Battin, J. Fellman, S. O'Neel, and R. G. M. Spencer (2015), Storage and release of organic carbon from glaciers and ice sheets, *Nature Geosci*, *8*(2), 91-96.

Hood, E., J. Fellman, R. G. M. Spencer, P. J. Hernes, R. Edwards, D. D'Amore, and D. Scott (2009), Glaciers as a source of ancient and labile organic matter to the marine environment, *Nature*, *462*(7276).

Hopkins, D. W., P. G. Dennis, S. P. Rushton, K. K. Newsham, and T. G. O'Donnell (2021), Lean and keen: Microbial activity in soils from the Maritime Antarctic, *Eur J Soil Sci*, *72*(1), 413-431.

Hopwood, M. J., D. P. Connelly, K. E. Arendt, T. Juul-Pedersen, M. Stinchcombe, L. Meire, M. Esposito, and R. Krishna (2016), Seasonal changes in Fe along a glaciated Greenlandic fjord, *Frontiers in Earth Science*, *4*, Doi:10.3389/feart.2016.00015.

Hopwood, M. J., et al. (2020), Review article: How does glacier discharge affect marine biogeochemistry and primary production in the Arctic?, *The Cryosphere*, *14*(4), 1347-1383.

Horikawa, T., D. Nomura, N. Kanna, Y. Fukamachi, and S. Sugiyama (2022), Effects of the glacial meltwater supply on carbonate chemistry in Bowdoin Fjord, Northwestern Greenland, *Frontiers in Marine Science*, *9*.

How, P., et al. (2021), Greenland-wide inventory of ice marginal lakes using a multi-method approach, *Scientific Reports*, *11*(1), 4481.

Hugelius, G., C. Tarnocai, G. Broll, J. G. Canadell, P. Kuhry, and D. K. Swanson (2013a), The Northern Circumpolar Soil Carbon Database: spatially distributed datasets of soil coverage and soil carbon storage in the northern permafrost regions, *Earth Syst. Sci. Data*, *5*(1), 3-13.

Hugelius, G., et al. (2014), Estimated stocks of circumpolar permafrost carbon with quantified uncertainty ranges and identified data gaps, *Biogeosciences*, *11*(23), 6573-6593.

Hugelius, G., et al. (2013b), A new data set for estimating organic carbon storage to 3 m depth in soils of the northern circumpolar permafrost region, *Earth Syst. Sci. Data*, *5*(2), 393-402.

Hughes, K. A., P. Convey, and J. Turner (2021), Developing resilience to climate change impacts in Antarctica: An evaluation of Antarctic Treaty System protected area policy, *Environmental Science & Policy*, *124*, 12-22.

IPCC (2006), 2006 IPCC Guidelines for National Greenhouse Gas Inventories*Rep.*, IGES, Japan.

James, R. H., et al. (2016), Effects of climate change on methane emissions from seafloor sediments in the Arctic Ocean: A review, *Limnol Oceanogr*, *61*(S1), S283-S299.

Kähler, P., P. K. Bjornsen, K. Lochte, and A. Antia (1997), Dissolved organic matter and its utilization by bacteria during spring in the Southern Ocean, *Deep Sea Research Part II: Topical Studies in Oceanography*, *44*(1), 341-353.

Kellerman, A. M., J. Vonk, S. McColaugh, D. C. Podgorski, E. van Winden, J. R. Hawkings, S. E. Johnston, M. Humayun, and R. G. M. Spencer (2021), Molecular Signatures of Glacial Dissolved Organic Matter From Svalbard and Greenland, *Global Biogeochem Cy*, *35*(3), e2020GB006709.

Keppler, L., P. Landschützer, N. Gruber, S. K. Lauvset, and I. Stemmler (2020), Seasonal Carbon Dynamics in the Near-Global Ocean, *Global Biogeochem Cy*, *34*(12), e2020GB006571.

Kierdorf, C. (2006), Variability of organic carbon along the ice-covered polar continental margin of East Greenland, 241 pp, University of Bremen, Bremen.

Kingston, J. (1992), The Undiscovered Oil and Gas of Antarctica*Rep.*, 77 pp, Santa Barbara, California.

Kleber, G. E., A. J. Hodson, L. Magerl, E. S. Mannerfelt, H. J. Bradbury, Y. Zhu, M. Trimmer, and A. V. Turchyn (2023), Groundwater springs formed during glacial retreat are a large source of methane in the high Arctic, *Nat Geosci*, *16*(7), 597-604.

Kleber, G. E., L. Magerl, A. V. Turchyn, K. Redeker, S. Thiele, M. Liira, K. Herodes, L. Øvreås, and A. Hodson (2024), Shallow and deep groundwater moderate methane dynamics in a high Arctic glacial catchment, *Frontiers in Earth Science*, *12*.

Kohler, T., J. D. Zarsky, J. C. Yde, G. Lamarche-Gagnon, J. Hawkings, A. Tedstone, J. L. Wadham, J. Box, A. Beaton, and M. Stibal (2017), Carbon dating reveals a seasonal progression in the source of particulate organic carbon exported from the Greenland Ice Sheet, *Geophys Res Lett*.

Kretschmer, K., A. Biastoch, L. Rüpke, and E. Burwicz (2015), Modeling the fate of methane hydrates under global warming, *Global Biogeochem Cy*, *29*(5), 610-625.

Krumhardt, K. M., M. C. Long, K. Lindsay, and M. N. Levy (2020), Southern Ocean Calcification Controls the Global Distribution of Alkalinity, *Global Biogeochem Cy*, *34*(12), e2020GB006727.

Kuhn, M. A., R. K. Varner, D. Bastviken, P. Crill, S. MacIntyre, M. Turetsky, K. Walter Anthony, A. D. McGuire, and D. Olefeldt (2021), BAWLD-CH4: a comprehensive dataset of methane fluxes from boreal and arctic ecosystems, *Earth Syst. Sci. Data*, *13*(11), 5151-5189.

Kulessa, B., et al. (2017), Seismic evidence for complex sedimentary control of Greenland Ice Sheet flow, *Science Advances*, *3*(8), e1603071.

Lamarche-Gagnon, G., J. R. Hawkings, and J. L. Wadham (2022a), Hydrochemistry of the Leverett Glacier proglacial river, Southwest Greenland (2009-2012) (Version 1) edited, Zenodo.

Lamarche-Gagnon, G., T. Kohler, E. Lawson, J. R. Hawkings, M. Stibal, and J. L. Wadham (2022b), Particulate organic carbon (POC) concentration in meltwater runoff of Leverett Glacier, Russell Glacier, and Isunnguata Sermia, southwest Greenland (2009-2018) (Version 2), edited, Zenodo.

Lamarche-Gagnon, G., et al. (2019), Greenland melt drives continuous export of methane from the ice-sheet bed, *Nature*, *565*(7737), 73-77.

Lancelot, C., A. de Montety, H. Goosse, S. Becquevort, V. Schoemann, B. Pasquer, and M. Vancoppenolle (2009), Spatial distribution of the iron supply to phytoplankton in the Southern Ocean: a model study, *Biogeosciences*, *6*(12), 2861-2878.

Laruelle, G. G., R. Lauerwald, B. Pfeil, and P. Regnier (2014), Regionalized global budget of the CO2 exchange at the air-water interface in continental shelf seas, *Global Biogeochem Cy*, *28*(11), 1199-1214.

Laruelle, G. G., P. Landschützer, N. Gruber, J. L. Tison, B. Delille, and P. Regnier (2017), Global high-resolution monthly pCO2 climatology for the coastal ocean derived from neural network interpolation, *Biogeosciences*, *14*(19), 4545-4561.

Laufkötter, C., A. A. Stern, J. G. John, C. A. Stock, and J. P. Dunne (2018), Glacial Iron Sources Stimulate the Southern Ocean Carbon Cycle, *Geophys Res Lett*, *45*(24), 13,377-313,385.

Lauvset, S. K., et al. (2021), An updated version of the global interior ocean biogeochemical data product, GLODAPv2.2021, *Earth Syst. Sci. Data*, *13*(12), 5565-5589.

Lawson, E., J. L. Wadham, M. Tranter, M. Stibal, G. Lis, C. Butler, J. Laybourn-Parry, P. Nienow, D. Chandler, and P. Dewsbury (2014), Greenland Ice Sheets exports labile organic carbon to the Arctic oceans, *Biogeosciences Discussions*, *10*, 19311–19345.

Lawson, E. C., J. L. Wadham, M. Tranter, M. Stibal, G. P. Lis, C. E. H. Butler, J. Laybourn-Parry, P. Nienow, D. Chandler, and P. Dewsbury (2014), Greenland Ice Sheet exports labile organic carbon to the Arctic oceans, *Biogeosciences*, *11*(14), 4015-4028.

Liljedahl, L. C., et al. (2021), Rapid and sensitive response of Greenland's groundwater system to ice sheet change, *Nat Geosci*, *14*(10), 751-755.

Liu, S., et al. (2022), The importance of hydrology in routing terrestrial carbon to the atmosphere via global streams and rivers, *Proceedings of the National Academy of Sciences*, *119*(11), e2106322119.

Lønborg, C., C. Carreira, T. Jickells, and X. A. Álvarez-Salgado (2020), Impacts of Global Change on Ocean Dissolved Organic Carbon (DOC) Cycling, *Frontiers in Marine Science*, *7*.

Luo, H., R. M. Castelao, A. K. Rennermalm, M. Tedesco, A. Bracco, Patricia L. Yager, and T. L. Mote (2016), Oceanic transport of surface meltwater from the southern Greenland ice sheet, *Nat Geosci*, *9*(7), 528-532.

MacGregor, J. A., et al. (2016), A synthesis of the basal thermal state of the Greenland Ice Sheet, *Journal of Geophysical Research: Earth Surface*, *121*(7), 1328-1350.

Maier, N., F. Gimbert, F. Gillet-Chaulet, and A. Gilbert (2021), Basal traction mainly dictated by hard-bed physics over grounded regions of Greenland, *The Cryosphere*, *15*(3), 1435-1451.

Manger, G. E. (1963), Porosity and bulk density of sedimentary rocks*Rep.*

Mankoff, K. D., B. Noël, X. Fettweis, A. P. Ahlstrøm, W. Colgan, K. Kondo, K. Langley, S. Sugiyama, D. van As, and R. S. Fausto (2020), Greenland liquid water discharge from 1958 through 2019, *Earth Syst. Sci. Data*, *12*(4), 2811-2841.

Masson-Delmotte, V., et al. (2012), Greenland climate change: from the past to the future, *WIREs Climate Change*, *3*(5), 427-449.

Matthews, E., M. S. Johnson, V. Genovese, J. Du, and D. Bastviken (2020), Methane emission from high latitude lakes: methane-centric lake classification and satellite-driven annual cycle of emissions, *Scientific Reports*, *10*(1), 12465.

Mau, S., et al. (2017), Widespread methane seepage along the continental margin off Svalbard - from Bjørnøya to Kongsfjorden, *Scientific Reports*, *7*(1), 42997.

Maule, C. F., M. E. Purucker, N. Olsen, and K. Mosegaard (2005), Heat flux anomalies in Antarctica revealed by satellite magnetic data, *Science*, *309*(5733), 464-467.

Meire, L., D. H. Søgaard, J. Mortensen, F. J. R. Meysman, K. Soetaert, K. E. Arendt, T. Juul-Pedersen, M. E. Blicher, and S. Rysgaard (2015), Glacial meltwater and primary production are drivers of strong CO2 uptake in fjord and coastal waters adjacent to the Greenland Ice Sheet, *Biogeosciences*, *12*(8), 2347-2363.

Meire, L., J. Mortensen, P. Meire, T. Juul-Pedersen, M. K. Sejr, S. Rysgaard, R. Nygaard, P. Huybrechts, and F. J. R. Meysman (2017), Marine-terminating glaciers sustain high productivity in Greenland fjords, *Global Change Biology*, Doi:10.1111/gcb.13801.

Meredith, M., et al. (2019), Polar Regions, in *IPCC Special Report on the Ocean and Cryosphere in a Changing Climate*, edited by H. O. Pörtner, et al., p. 118.

Messager, M. L., B. Lehner, G. Grill, I. Nedeva, and O. Schmitt (2016), Estimating the volume and age of water stored in global lakes using a geo-statistical approach, *Nat Comms*, *7*(1), 13603.

Michaud, A. B., M. L. Skidmore, A. C. Mitchell, T. J. Vick-Majors, C. Barbante, C. Turetta, W. vanGelder, and J. C. Priscu (2016), Solute sources and geochemical processes in Subglacial Lake Whillans, West Antarctica, *Geology*, Doi:10.1130/g37639.37631.

Michaud, A. B., J. E. Dore, A. M. Achberger, B. C. Christner, A. C. Mitchell, M. L. Skidmore, T. J. Vick-Majors, and J. C. Priscu (2017), Microbial oxidation as a methane sink beneath the West Antarctic Ice Sheet, *Nature Geosci*, *10*(8), 582-586.

Mikaloff Fletcher, S. E., et al. (2007), Inverse estimates of the oceanic sources and sinks of natural CO2 and the implied oceanic carbon transport, *Global Biogeochem Cy*, *21*(1).

Mikucki, J. A., E. Auken, S. Tulaczyk, R. A. Virginia, C. Schamper, K. I. Sorensen, P. T. Doran, H. Dugan, and N. Foley (2015), Deep groundwater and potential subsurface habitats beneath an Antarctic dry valley, *Nat Commun*, *6*.

Miteva, V., C. Teacher, T. Sowers, and J. Brenchley (2009), Comparison of the microbial diversity at different depths of the GISP2 Greenland ice core in relationship to deposition climates, *Environmental Microbiology*, *11*(3), 640-656.

Møller, E. F., A. Christensen, J. Larsen, K. D. Mankoff, M. H. Ribergaard, M. K. Sejr, P. Wallhead, and M. Maar (2022), The sensitivity of primary productivity in Disko Bay, a coastal Arctic ecosystem to changes in freshwater discharge and sea ice cover, *EGUsphere*, *2022*, 1-52.

Mongwe, P., L. Gregor, J. Tjiputra, J. Hauck, T. Ito, C. Danek, M. Vichi, S. Thomalla, and P. M. S. Monteiro (2024), Projected poleward migration of the Southern Ocean CO2 sink region under high emissions, *Communications Earth & Environment*, *5*(1), 232.

Moon, S., C. P. Chamberlain, and G. E. Hilley (2014), New estimates of silicate weathering rates and their uncertainties in global rivers, *Geochim Cosmochim Ac*, *134*, 257-274.

Moon, T., M. Fisher, L. Harden, and T. Stafford (2021), QGreenland (v1.0.0) (software), edited by N. S. a. I. D. Center.

Morlighem, M., et al. (2017), BedMachine v3: Complete Bed Topography and Ocean Bathymetry Mapping of Greenland From Multibeam Echo Sounding Combined With Mass Conservation, *Geophys Res Lett*, *44*(21), 11,051-011,061.

Nielsen, T., T. Laier, A. Kuijpers, T. L. Rasmussen, N. E. Mikkelsen, and N. Nørgård-Pedersen (2014), Fluid flow and methane occurrences in the Disko Bugt area offshore West Greenland: indications for gas hydrates?, *Geo-Mar Lett*, *34*(6), 511-523.

Nissen, C., R. Timmermann, M. Hoppema, Ö. Gürses, and J. Hauck (2022), Abruptly attenuated carbon sequestration with Weddell Sea dense waters by 2100, *Nat Comms*, *13*(1), 3402.

O'Donnell, E. C., J. L. Wadham, G. P. Lis, M. Tranter, A. E. Pickard, M. Stibal, P. Dewsbury, and S. Fitzsimons (2016), Identification and analysis of low-molecular-weight dissolved organic carbon in subglacial basal ice ecosystems by ion chromatography, *Biogeosciences*, *13*(12), 3833-3846.

Ogawa, H., R. Fukuda, and I. Koike (1999), Vertical distributions of dissolved organic carbon and nitrogen in the Southern Ocean, *Deep Sea Research Part I: Oceanographic Research Papers*, *46*(10), 1809-1826.

Oksman, M., et al. (2022), Impact of freshwater runoff from the southwest Greenland Ice Sheet on fjord productivity since the late 19th century, *The Cryosphere*, *16*(6), 2471-2491.

Olafsson, J., S. R. Olafsdottir, T. Takahashi, M. Danielsen, and T. S. Arnarson (2021), Enhancement of the North Atlantic CO2 sink by Arctic Waters, *Biogeosciences*, *18*(5), 1689-1701.

Oliver, H., et al. (2018), Exploring the Potential Impact of Greenland Meltwater on Stratification, Photosynthetically Active Radiation, and Primary Production in the Labrador Sea, *Journal of Geophysical Research: Oceans*, *123*(4), 2570-2591.

Overduin, P. P., T. Schneider von Deimling, F. Miesner, M. N. Grigoriev, C. Ruppel, A. Vasiliev, H. Lantuit, B. Juhls, and S. Westermann (2019), Submarine Permafrost Map in the Arctic Modeled Using 1-D Transient Heat Flux (SuPerMAP), *Journal of Geophysical Research: Oceans*, *124*(6), 3490-3507.

Overeem, I., B. D. Hudson, J. P. M. Syvitski, A. B. Mikkelsen, B. Hasholt, M. R. van den Broeke, B. P. Y. Noël, and M. Morlighem (2017), Substantial export of suspended sediment to the global oceans from glacial erosion in Greenland, *Nat Geosci*, *10*, 859.

Pain, A. J., J. B. Martin, E. E. Martin, S. Rahman, and P. Ackermann (2020), Differences in the Quantity and Quality of Organic Matter Exported From Greenlandic Glacial and Deglaciated Watersheds, *Global Biogeochem Cy*, *34*(10), e2020GB006614.

Pain, A. J., J. B. Martin, E. E. Martin, Å. K. Rennermalm, and S. Rahman (2021), Heterogeneous CO2 and CH4 content of glacial meltwater from the Greenland Ice Sheet and implications for subglacial carbon processes, *The Cryosphere*, *15*(3), 1627-1644.

Parkhurst, D., and C. A. J. Appelo (2013), Description of input and examples for PHREEQC version 3–A computer program for speciation, batch-reaction, one-dimensional transport, and inverse geochemical calculations, in *Techniques and Methods*, edited, USGS.

Parmentier, F.-J. W., T. R. Christensen, S. Rysgaard, J. Bendtsen, R. N. Glud, B. Else, J. van Huissteden, T. Sachs, J. E. Vonk, and M. K. Sejr (2017), A synthesis of the arctic terrestrial and marine carbon cycles under pressure from a dwindling cryosphere, *Ambio*, *46*(1), 53-69.

Paulsen, M. L., et al. (2017), Carbon Bioavailability in a High Arctic Fjord Influenced by Glacial Meltwater, NE Greenland, *Frontiers in Marine Science*, *4*.

Paxman, G. J. G., J. Austermann, and K. J. Tinto (2021), A fault-bounded palaeo-lake basin preserved beneath the Greenland Ice Sheet, *Earth Planet Sc Lett*, *553*, 116647.

Peng, S., and J. Zhang (2007), *Engineering geology for underground rocks*, Springer Science & Business Media.
.

Peng, T. H., and T. Takahashi (1993), Ocean uptake of carbon dioxide, in *National conference and exposition on heat transfer*, edited, pp. 2-9, Atlanta, GA (United States).

Pérez, F. F., et al. (2024), An Assessment of CO2 Storage and Sea-Air Fluxes for the Atlantic Ocean and Mediterranean Sea Between 1985 and 2018, *Global Biogeochem Cy*, *38*(4), e2023GB007862.

Perner, K., M. Moros, O. H. Otterå, T. Blanz, R. R. Schneider, and E. Jansen (2019), An oceanic perspective on Greenland's recent freshwater discharge since 1850, *Scientific Reports*, *9*(1), 17680.

Person, R., O. Aumont, G. Madec, M. Vancoppenolle, L. Bopp, and N. Merino (2019), Sensitivity of ocean biogeochemistry to the iron supply from the Antarctic Ice Sheet explored with a biogeochemical model, *Biogeosciences*, *16*(18), 3583-3603.

Pinkerton, M. H., P. W. Boyd, S. Deppeler, A. Hayward, J. Höfer, and S. Moreau (2021), Evidence for the Impact of Climate Change on Primary Producers in the Southern Ocean, *Frontiers in Ecology and Evolution*, *9*.

Pires, C. V., C. E. R. G. Schaefer, A. K. Hashigushi, A. Thomazini, E. I. F. Filho, and E. S. Mendonça (2017), Soil organic carbon and nitrogen pools drive soil C-CO2 emissions from selected soils in Maritime Antarctica, *Sci Total Environ*, *596-597*, 124-135.

Portal, G. R. A. D. (2022), edited, Greenland Resource Assessment Data Portal https://greenland-resource-assessment.gl.

Porter, C., et al. (2018), ArcticDEM, Version 3, edited, Harvard Dataverse.

Pötter, L., R. Tollrian, F. Wisotzky, and L. C. Weiss (2021), Determining freshwater pCO2 based on geochemical calculation and modelling using PHREEQC, *MethodsX*, *8*, 101430.

Ramage, J., et al. (2024), The net GHG balance and budget of the permafrost region (2000–2020) from ecosystem flux upscaling, *Global Biogeochem. Cycles*, *38*.

Rantanen, M., A. Y. Karpechko, A. Lipponen, K. Nordling, O. Hyvärinen, K. Ruosteenoja, T. Vihma, and A. Laaksonen (2022), The Arctic has warmed nearly four times faster than the globe since 1979, *Communications Earth & Environment*, *3*(1), 168.

Reynolds, P., S. Planke, J. M. Millett, D. A. Jerram, M. Trulsvik, N. Schofield, and R. Myklebust (2017), Hydrothermal vent complexes offshore Northeast Greenland: A potential role in driving the PETM, *Earth Planet Sc Lett*, *467*, 72-78.

Rosentreter, J. A., et al. (2021), Half of global methane emissions come from highly variable aquatic ecosystem sources, *Nat Geosci*, *14*(4), 225-230.

Rosentreter, J. A., et al. (2023), Coastal vegetation and estuaries are collectively a greenhouse sink, *Nature Climate Change*, *13*, 579-587.

Ruben, M., J. Hefter, F. Schubotz, W. Geibert, M. Butzin, T. Gentz, H. Grotheer, M. Forwick, W. Szczuciński, and G. Mollenhauer (2023), Fossil organic carbon utilization in marine Arctic fjord sediments by subsurface micro-organisms, *Nat Geosci*, *16*(7), 625-630.

Ruiz-Halpern, S., M. K. Sejr, C. M. Duarte, D. Krause-Jensen, T. Dalsgaard, J. Dachs, and S. Rysgaard (2010), Air-water exchange and vertical profiles of organic carbon in a subarctic fjord, *Limnol Oceanogr*, *55*(4), 1733-1740.

Ruppel, C. D., and J. D. Kessler (2017), The interaction of climate change and methane hydrates, *Rev Geophys*, *55*(1), 126-168.

Rysgaard, S., J. Bendtsen, J. Mortensen, and M. K. Sejr (2018), High geothermal heat flux in close proximity to the Northeast Greenland Ice Stream, *Scientific Reports*, *8*(1), 1344.

Rysgaard, S., J. Bendtsen, L. T. Pedersen, H. Ramløv, and R. N. Glud (2009), Increased CO2 uptake due to sea ice growth and decay in the Nordic Seas, *Journal of Geophysical Research: Oceans*, *114*(C9).

Rysgaard, S., J. Mortensen, T. Juul-Pedersen, L. L. Sørensen, K. Lennert, D. H. Søgaard, K. E. Arendt, M. E. Blicher, M. K. Sejr, and J. Bendtsen (2012), High air–sea CO2 uptake rates in nearshore and shelf areas of Southern Greenland: Temporal and spatial variability, *Mar Chem*, *128-129*, 26-33.

Sachs, O., E. J. Sauter, M. Schlüter, M. M. Rutgers van der Loeff, K. Jerosch, and O. Holby (2009), Benthic organic carbon flux and oxygen penetration reflect different plankton provinces in the Southern Ocean, *Deep Sea Research Part I: Oceanographic Research Papers*, *56*(8), 1319-1335.

Saros, J. E., C. L. Osburn, R. M. Northington, S. D. Birkel, J. D. Auger, C. A. Stedmon, and N. J. Anderson (2015), Recent decrease in DOC concentrations in Arctic lakes of southwest Greenland, *Geophys Res Lett*, *42*(16), 6703-6709.

Saunois, M., et al. (2020), The Global Methane Budget 2000–2017, *Earth Syst. Sci. Data*, *12*(3), 1561-1623.

Seabrook, S., C. S. Law, A. R. Thurber, Y. Ladroit, V. Cummings, L. Tait, A. Maurice, and I. Hawes (2025), Antarctic seep emergence and discovery in the shallow coastal environment, *Nat Comms*, *16*(1), 8740.

Seifert, M., et al. (2019), Influence of Glacial Meltwater on Summer Biogeochemical Cycles in Scoresby Sund, East Greenland, *Frontiers in Marine Science*, *6*.

Serov, P., et al. (2017), Postglacial response of Arctic Ocean gas hydrates to climatic amelioration, *Proceedings of the National Academy of Sciences*, *114*(24), 6215-6220.

Shadwick, E. H., O. A. De Meo, S. Schroeter, M. C. Arroyo, D. G. Martinson, and H. Ducklow (2021), Sea Ice Suppression of CO2 Outgassing in the West Antarctic Peninsula: Implications For The Evolving Southern Ocean Carbon Sink, *Geophys Res Lett*, *48*(11), e2020GL091835.

Siegert, M. J., N. Ross, and A. M. L. Brocq (2016), Recent advances in understanding Antarctic subglacial lakes and hydrology, *Phil. Trans. Royal Soc. A*, *374*(2059), Doi:10.1098/rsta.2014.0306.

Siegert, M. J., B. Kulessa, M. Bougamont, P. Christoffersen, K. Key, K. R. Andersen, A. D. Booth, and A. M. Smith (2018), Antarctic subglacial groundwater: a concept paper on its measurement and potential influence on ice flow, *Geological Society, London, Special Publications*, *461*(1), 197.

Slater, T., et al. (2021), Increased variability in Greenland Ice Sheet runoff from satellite observations, *Nat Comms*, *12*(1), 6069.

Smith, R. W., T. S. Bianchi, M. Allison, C. Savage, and V. Galy (2015), High rates of organic carbon burial in fjord sediments globally, *Nature Geosci*, *8*(6), 450-453.

Sørensen, H. L., L. Meire, T. Juul-Pedersen, H. C. de Stigter, F. J. R. Meysman, S. Rysgaard, B. Thamdrup, and R. N. Glud (2015), Seasonal carbon cycling in a Greenlandic fjord: an integrated pelagic and benthic study, *Mar Ecol Prog Ser*, *539*, 1-17.

Souchez, R., J. Jouzel, A. Landais, J. Chappellaz, R. Lorrain, and J. L. Tison (2006), Gas isotopes in ice reveal a vegetated central Greenland during ice sheet invasion, *Geophys Res Lett*, *33*(24), -.

Soulet, G., R. G. Hilton, M. H. Garnett, T. Roylands, S. Klotz, T. Croissant, M. Dellinger, and C. Le Bouteiller (2021), Temperature control on CO2 emissions from the weathering of sedimentary rocks, *Nat Geosci*, *14*(9), 665-671.

St John, B. (1986), Antarctica - Geology and hydrocarbon potential, in *Future petroleum provinces of the world: American Association of Petroleum Geologists Memoir* edited by A. A. o. P. Geologists, pp. 55-100.

St. Pierre, K. A., V. L. St. Louis, S. L. Schiff, I. Lehnherr, P. G. Dainard, A. S. Gardner, P. J. K. Aukes, and M. J. Sharp (2019), Proglacial freshwaters are significant and previously unrecognized sinks of atmospheric CO<sub>2</sub&gt, *Proceedings of the National Academy of Sciences*, *116*(36), 17690.

Stanley, E. H., N. J. Casson, S. T. Christel, J. T. Crawford, L. C. Loken, and S. K. Oliver (2016), The ecology of methane in streams and rivers: patterns, controls, and global significance, *Ecol Monogr*, *86*(2), 146-171.

Stibal, M., M. Sebacka, and J. D. Zarsky (2012a), Biological processes on glacier and ice sheet surfaces, *Nat Geosci*.

Stibal, M., F. Hasan, J. L. Wadham, M. J. Sharp, and A. M. Anesio (2012b), Prokaryotic diversity in sediments beneath two polar glaciers with contrasting organic carbon substrates, *Extremophiles*, *16*(2), 255-265.

Stolpmann, L., et al. (2021), First pan-Arctic assessment of dissolved organic carbon in lakes of the permafrost region, *Biogeosciences*, *18*(12), 3917-3936.

Takahashi, T., et al. (2002), Global sea–air CO2 flux based on climatological surface ocean pCO2, and seasonal biological and temperature effects, *Deep Sea Research Part II: Topical Studies in Oceanography*, *49*(9), 1601-1622.

Takahashi, T., et al. (2009), Climatological mean and decadal change in surface ocean pCO2, and net sea–air CO2 flux over the global oceans, *Deep Sea Research Part II: Topical Studies in Oceanography*, *56*(8), 554-577.

Telling, J., et al. (2015), Rock comminution as a source of hydrogen for subglacial ecosystems, *Nature Geosci*, *8*(11), 851-855.

Thomazini, A., et al. (2015), CO2 and N2O emissions in a soil chronosequence at a glacier retreat zone in Maritime Antarctica, *Sci Total Environ*, *521-522*, 336-345.

Thurber, A. R., S. Seabrook, and R. M. Welsh (2020), Riddles in the cold: Antarctic endemism and microbial succession impact methane cycling in the Southern Ocean, *Proceedings of the Royal Society B: Biological Sciences*, *287*(1931), 20201134.

USGS (2008), Geochemistry of rock samples from the National Geochemical Database, edited by U. S. G. Survey, Veston, VA.

Vonk, J. E., et al. (2025), The land–ocean Arctic carbon cycle, *Nature Reviews Earth & Environment*, *6*(2), 86-105.

Vrbická, K., et al. (2022), Catchment characteristics and seasonality control the composition of microbial assemblages exported from three outlet glaciers of the Greenland Ice Sheet, *Front Microbiol*.

Wadham, J. L., M. Tranter, S. Tulaczyk, and M. Sharp (2008), Subglacial methanogenesis: A potential climatic amplifier?, *Global Biogeochem. Cycles*, *22*(2), GB2021.

Wadham, J. L., J. R. Hawkings, L. Tarasov, L. J. Gregoire, R. G. M. Spencer, M. Gutjahr, A. Ridgwell, and K. E. Kohfeld (2019), Ice sheets matter for the global carbon cycle, *Nat Comms*, *10*(1), 3567.

Wadham, J. L., et al. (2012), Potential methane reservoirs beneath Antarctica, *Nature*, *488*(7413), 633-637.

Walsh, E. V., R. G. Hilton, S. E. Tank, and E. Amos (2024), Temperature sensitivity of the mineral permafrost feedback at the continental scale, *Science Advances*, *10*(41), eadq4893.

Walter Anthony, K. M., P. Anthony, G. Grosse, and J. Chanton (2012), Geologic methane seeps along boundaries of Arctic permafrost thaw and melting glaciers, *Nat Geosci*, *5*(6), 419-426.

Walter, F., J. Chaput, and M. P. Lüthi (2014), Thick sediments beneath Greenland's ablation zone and their potential role in future ice sheet dynamics, *Geology*, *42*(6), 487-490.

Weitemeyer, K. A., and B. A. Buffett (2006), Accumulation and release of methane from clathrates below the Laurentide and Cordilleran ice sheets, *Global and Planetary Change*, *53*(3), 176-187.

Wu, Y., M. P. Hain, M. P. Humphreys, S. Hartman, and T. Tyrrell (2019), What drives the latitudinal gradient in open-ocean surface dissolved inorganic carbon concentration?, *Biogeosciences*, *16*(13), 2661-2681.

Yang, Q., T. H. Dixon, P. G. Myers, J. Bonin, D. Chambers, M. R. van den Broeke, M. H. Ribergaard, and J. Mortensen (2016), Recent increases in Arctic freshwater flux affects Labrador Sea convection and Atlantic overturning circulation, *Nat Comms*, *7*(1), 10525.

Yasunaka, S., et al. (2023), An assessment of sea-air CO2 flux in the Arctic Ocean from 1985 to 2018, *Global Biogeochem. Cycles*, *37*.

Yde, J. C., K. W. Finster, R. Raiswell, J. P. Steffensen, J. Heinemeier, J. Olsen, H. P. Gunnlaugsson, and O. B. Nielsen (2010), Basal ice microbiology at the margin of the Greenland ice sheet, *Annals of Glaciology*, *51*(56), 71-79.

Zeebe, R. E. (2012), History of Seawater Carbonate Chemistry, Atmospheric CO2, and Ocean Acidification, *Annual Review of Earth and Planetary Sciences*, *40*(Volume 40, 2012), 141-165.

Zemskova, V. E., T.-L. He, Z. Wan, and N. Grisouard (2022), A deep-learning estimate of the decadal trends in the Southern Ocean carbon storage, *Nat Comms*, *13*(1), 4056.

Zeng, N. (2003), Glacial-interglacial atmospheric CO2 change —The glacial burial hypothesis, *Advances in Atmospheric Sciences*, *20*(5), 677-693.

Zolkos, S., S. E. Tank, and S. V. Kokelj (2018), Mineral Weathering and the Permafrost Carbon-Climate Feedback, *Geophys Res Lett*, *45*(18), 9623-9632.

Zondervan, J. R., R. G. Hilton, M. Dellinger, F. J. Clubb, T. Roylands, and M. Ogrič (2023), Rock organic carbon oxidation CO2 release offsets silicate weathering sink, *Nature*, *623*(7986), 329-333.

Additional Supplementary References

Arndt, S., B. B. Jørgensen, D. LaRowe, J. Middelburg, R. Pancost, and P. Regnier (2013), Quantifying the degradation of organic matter in marine sediments: A review and synthesis, *Earth-Sci Rev*, *123*, 53-86.

Athy, L. F. (1930), Density, Porosity and Compaction of Sedimentary Rocks*Rep.*, 1-24 pp.

Aumont, O., C. Ethé, A. Tagliabue, L. Bopp, and M. Gehlen (2015), PISCES-v2: an ocean biogeochemical model for carbon and ecosystem studies, *Geosci. Model Dev.*, *8*(8), 2465-2513.

Berner, R. A. (1980), *Early Diagenesis: A Theoretical Approach*, 241 pp., Princeton University Press, Princeton.

Boudreau, B. P. (Ed.) (1997), *Diagenetic models and their implementation: modeling transport and reactions in aquatic sediments*, 414 pp., Springer.

Bradley, J. A., D. Hülse, D. E. LaRowe, and S. Arndt (2022), Transfer efficiency of organic carbon in marine sediments, *Nat Comms*, *13*(1), 7297.

Brodersen, K. P., and N. J. Anderson (2002), Distribution of chironomids (Diptera) in low arctic West Greenland lakes: trophic conditions, temperature and environmental reconstruction, *Freshwater Biology*, *47*(6), 1137-1157.

Bushinsky, S. M., P. Landschützer, C. Rödenbeck, A. R. Gray, D. Baker, M. R. Mazloff, L. Resplandy, K. S. Johnson, and J. L. Sarmiento (2019), Reassessing Southern Ocean Air-Sea CO2 Flux Estimates With the Addition of Biogeochemical Float Observations, *Global Biogeochem Cy*, *33*(11), 1370-1388.

Calmels, D., J. r. m. Gaillardet, A. s. Brenot, and C. France-Lanord (2007), Sustained sulfide oxidation by physical erosion processes in the Mackenzie River basin: Climatic perspectives, *Geology*, *35*(11), 1003-1006.

Chau, T. T. T., M. Gehlen, and F. Chevallier (2022), A seamless ensemble-based reconstruction of surface ocean pCO2 and air–sea CO2 fluxes over the global coastal and open oceans, *Biogeosciences*, *19*(4), 1087-1109.

Christner, B. C., G. G. Montross, and J. C. Priscu (2012), Dissolved gases in frozen basal water from the NGRIP borehole: implications for biogeochemical processes beneath the Greenland Ice Sheet, *Polar Biology*, *35*(11), 1735-1741.

Chu, V. W. (2014), Greenland ice sheet hydrology:A review, *Progress in Physical Geography: Earth and Environment*, *38*(1), 19-54.

Ciais, P., et al. (2022), Definitions and methods to estimate regional land carbon fluxes for the second phase of the REgional Carbon Cycle Assessment and Processes Project (RECCAP-2), *Geosci. Model Dev.*, *15*(3), 1289-1316.

Copard, Y., P. Amiotte-Suchet, and C. Di-Giovanni (2007), Storage and release of fossil organic carbon related to weathering of sedimentary rocks, *Earth Planet Sc Lett*, *258*(1), 345-357.

Dahl-Jensen, D., et al. (2013), Eemian interglacial reconstructed from a Greenland folded ice core, *Nature*, *493*(7433), 489-494.

Dalai, T. K., S. Krishnaswami, and M. M. Sarin (2002), Major ion chemistry in the headwaters of the Yamuna river system:: Chemical weathering, its temperature dependence and CO2 consumption in the Himalaya, *Geochim Cosmochim Ac*, *66*(19), 3397-3416.

Das, A., C.-H. Chung, and C.-F. You (2012), Disproportionately high rates of sulfide oxidation from mountainous river basins of Taiwan orogeny: Sulfur isotope evidence, *Geophys Res Lett*, *39*(12). Doi.org/10.1029/2012GL051549.

Delaigue, L., H. Thomas, and A. Mucci (2020), Spatial variations in CO2 fluxes in the Saguenay Fjord (Quebec, Canada) and results of a water mixing model, *Biogeosciences*, *17*(2), 547-566.

Doney, S. C., I. Lima, R. A. Feely, D. M. Glover, K. Lindsay, N. Mahowald, J. K. Moore, and R. Wanninkhof (2009), Mechanisms governing interannual variability in upper-ocean inorganic carbon system and air–sea CO2 fluxes: Physical climate and atmospheric dust, *Deep Sea Research Part II: Topical Studies in Oceanography*, *56*(8), 640-655.

Döscher, R., et al. (2022), The EC-Earth3 Earth system model for the Coupled Model Intercomparison Project 6, *Geosci. Model Dev.*, *15*(7), 2973-3020.

Dow, C. F., A. Hubbard, A. D. Booth, S. Doyle, A. Gusmeroli, and B. Kulessa (2013), Seismic evidence of mechanically weak sediments underlying Russell Glacier, West Greenland, *Annals of Glaciology*, *54*(64), 135-141.

Freitas, F. S., P. A. Pika, S. Kasten, B. B. Jørgensen, J. Rassmann, C. Rabouille, S. Thomas, H. Sass, R. D. Pancost, and S. Arndt (2021), New insights into large-scale trends of apparent organic matter reactivity in marine sediments and patterns of benthic carbon transformation, *Biogeosciences*, *18*(15), 4651-4679.

Galy, A., and C. France-Lanord (1999), Weathering processes in the Ganges–Brahmaputra basin and the riverine alkalinity budget, *Chem Geol*, *159*(1), 31-60.

Garcia-Tigreros Kodovska, F., K. J. Sparrow, S. A. Yvon-Lewis, A. Paytan, N. T. Dimova, A. Lecher, and J. D. Kessler (2016), Dissolved methane and carbon dioxide fluxes in Subarctic and Arctic regions: Assessing measurement techniques and spatial gradients, *Earth Planet Sc Lett*, *436*, 43-55.

Gloege, L., M. Yan, T. Zheng, and G. A. McKinley (2022), Improved Quantification of Ocean Carbon Uptake by Using Machine Learning to Merge Global Models and pCO2 Data, *Journal of Advances in Modeling Earth Systems*, *14*(2), e2021MS002620.

Gregor, L., A. D. Lebehot, S. Kok, and P. M. Scheel Monteiro (2019), A comparative assessment of the uncertainties of global surface ocean CO2 estimates using a machine-learning ensemble (CSIR-ML6 version 2019a) – have we hit the wall?, *Geosci. Model Dev.*, *12*(12), 5113-5136.

Harned, H. S., and R. Davis, Jr. (1943), The Ionization Constant of Carbonic Acid in Water and the Solubility of Carbon Dioxide in Water and Aqueous Salt Solutions from 0 to 50°, *Journal of the American Chemical Society*, *65*(10), 2030-2037.

Hauck, J., et al. (2020), Consistency and Challenges in the Ocean Carbon Sink Estimate for the Global Carbon Budget, *Frontiers in Marine Science*, *7*. DOI:10.3389/fmars.2020.571720.

Haumann, F. A., N. Gruber, M. Münnich, I. Frenger, and S. Kern (2016), Sea-ice transport driving Southern Ocean salinity and its recent trends, *Nature*, *537*(7618), 89-92.

Heginbottom, J. A., J. Brown, E. S. Melnikov, and O. J. Ferrians (1993), Circumarctic Map of Permafrost and Ground Ice Conditions, in *Permafrost: Sixth International Conference*, edited, pp. 1132-1136, South China University Press, Beijing, China.

Herron, S., u. Hoar, and C. C. Langway (1979), The Debris-Laden Ice at the Bottom of the Greenland Ice Sheet, *J Glaciol*, *23*(89), 193-207.

Hilton, R. G., J. Gaillardet, D. Calmels, and J.-L. Birck (2014), Geological respiration of a mountain belt revealed by the trace element rhenium, *Earth Planet Sc Lett*, *403*, 27-36.

Hjartarson, A., and H. Armannsson (2010), Geothermal research in Greenland, paper presented at Proceedings World Geothermal Congress International Geothermal Energy Association, Bali, Indonesia, 1-8.

Horan, K., R. G. Hilton, D. Selby, C. J. Ottley, D. R. Gröcke, M. Hicks, and K. W. Burton (2017), Mountain glaciation drives rapid oxidation of rock-bound organic carbon, *Science Advances*, *3*(10), e1701107.

Hülse, D., S. Arndt, S. Daines, P. Regnier, and A. Ridgwell (2018), OMEN-SED 1.0: a novel, numerically efficient organic matter sediment diagenesis module for coupling to Earth system models, *Geosci. Model Dev.*, *11*(7), 2649-2689.

Iida, Y., Y. Takatani, A. Kojima, and M. Ishii (2021), Global trends of ocean CO2 sink and ocean acidification: an observation-based reconstruction of surface ocean inorganic carbon variables, *Journal of Oceanography*, *77*(2), 323-358.

Kochtitzky, W., and L. Copland (2022), Retreat of Northern Hemisphere Marine-Terminating Glaciers, 2000–2020, *Geophys Res Lett*, *49*(3), e2021GL096501.

Krause-Jensen, D., N. Marbà, B. Olesen, M. K. Sejr, P. B. Christensen, J. Rodrigues, P. E. Renaud, T. J. S. Balsby, and S. Rysgaard (2012), Seasonal sea ice cover as principal driver of spatial and temporal variation in depth extension and annual production of kelp in Greenland, *Global Change Biology*, *18*(10), 2981-2994.

Kriest, I., and A. Oschlies (2015), MOPS-1.0: towards a model for the regulation of the global oceanic nitrogen budget by marine biogeochemical processes, *Geosci. Model Dev.*, *8*(9), 2929-2957.

Landschützer, P., N. Gruber, and D. C. E. Bakker (2016), Decadal variations and trends of the global ocean carbon sink, *Global Biogeochem Cy*, *30*(10), 1396-1417.

LaRowe, D. E., S. Arndt, J. A. Bradley, E. Burwicz, A. W. Dale, and J. P. Amend (2020), Organic carbon and microbial activity in marine sediments on a global scale throughout the Quaternary, *Geochim Cosmochim Ac*, *286*, 227-247.

Manning, C. C., V. L. Preston, S. F. Jones, A. P. M. Michel, D. P. Nicholson, P. J. Duke, M. M. M. Ahmed, K. Manganini, B. G. T. Else, and P. D. Tortell (2020), River Inflow Dominates Methane Emissions in an Arctic Coastal System, *Geophys Res Lett*, *47*(10), e2020GL087669.

Marienfeld, P. (1992), Sedimentology of the Scoresby Sund, East Greenland, in *Supplement to: Marienfeld, P (1992): Recent sedimentary processes in Scoresby Sund, East Greenland. Boreas, 21(2), 169-186, https://doi.org/10.1111/j.1502-3885.1992.tb00024.x*, edited, PANGAEA.

Märki, L., M. Lupker, C. France-Lanord, J. Lavé, S. Gallen, A. P. Gajurel, N. Haghipour, F. Leuenberger-West, and T. Eglinton (2021), An unshakable carbon budget for the Himalaya, *Nat Geosci*, *14*(10), 745-750.

Martos, Y. M., T. A. Jordan, M. Catalán, T. M. Jordan, J. L. Bamber, and D. G. Vaughan (2018), Geothermal Heat Flux Reveals the Iceland Hotspot Track Underneath Greenland, *Geophys Res Lett*, *45*(16), 8214-8222.

Mauritsen, T., et al. (2019), Developments in the MPI-M Earth System Model version 1.2 (MPI-ESM1.2) and Its Response to Increasing CO2, *Journal of Advances in Modeling Earth Systems*, *11*(4), 998-1038.

Nissen, C., M. Vogt, M. Münnich, N. Gruber, and F. A. Haumann (2018), Factors controlling coccolithophore biogeography in the Southern Ocean, *Biogeosciences*, *15*(22), 6997-7024.

Noël, B., W. J. v. d. Berg, S. Lhermitte, and M. R. v. d. Broeke (2019), Rapid ablation zone expansion amplifies north Greenland mass loss, *Science Advances*, *5*(9), eaaw0123.

Ogric, M. (2021), Chemical weathering of sedimentary rocks as a source of carbon dioxide to the atmosphere, Unpublished PhD Thesis, 239 pp, Durham University.

Olefeldt, D., et al. (2021), The Boreal–Arctic Wetland and Lake Dataset (BAWLD), *Earth Syst. Sci. Data*, *13*(11), 5127-5149.

Pika, P., D. Hülse, and S. Arndt (2021), OMEN-SED(-RCM) (v1.1): a pseudo-reactive continuum representation of organic matter degradation dynamics for OMEN-SED, *Geosci. Model Dev.*, *14*(11), 7155-7174.

Pika, P. A., D. Hülse, T. I. Eglinton, and S. Arndt (2023), Regional and Global Patterns of Apparent Organic Matter Reactivity in Marine Sediments, *Global Biogeochem Cy*, *37*(8), e2022GB007636.

Ribeiro, S., et al. (2017), Sea ice and primary production proxies in surface sediments from a High Arctic Greenland fjord: Spatial distribution and implications for palaeoenvironmental studies, *Ambio*, *46*(1), 106-118.

Rödenbeck, C., T. DeVries, J. Hauck, C. Le Quéré, and R. F. Keeling (2022), Data-based estimates of interannual sea–air CO2 flux variations 1957–2020 and their relation to environmental drivers, *Biogeosciences*, *19*(10), 2627-2652.

Ruskeeniemi, T., J. Engström, J. Lehtimäki, H. Vanhala, K. Korhonen, A. Kontula, L. Claesson Liljedahl, J.-O. Näslund, and R. Pettersson (2018), Subglacial permafrost evidencing re-advance of the Greenland Ice Sheet over frozen ground, *Quaternary Sci Rev*, *199*, 174-187.

Schaefer, J. M., R. C. Finkel, G. Balco, R. B. Alley, M. W. Caffee, J. P. Briner, N. E. Young, A. J. Gow, and R. Schwartz (2016), Greenland was nearly ice-free for extended periods during the Pleistocene, *Nature*, *540*(7632), 252-255.

Schenk, C. J. (2008), Geology and assessment of undiscovered oil and gas resources of the West Greenland-East Canada Province, *US Geological Survey Report 1824-J, 32pp.*

Schourup-Kristensen, V., D. Sidorenko, D. A. Wolf-Gladrow, and C. Völker (2014), A skill assessment of the biogeochemical model REcoM2 coupled to the Finite Element Sea Ice–Ocean Model (FESOM 1.3), *Geosci. Model Dev.*, *7*(6), 2769-2802.

Schourup-Kristensen, V., C. Wekerle, D. A. Wolf-Gladrow, and C. Völker (2018), Arctic Ocean biogeochemistry in the high resolution FESOM 1.4-REcoM2 model, *Prog Oceanogr*, *168*, 65-81.

Schwinger, J., N. Goris, J. F. Tjiputra, I. Kriest, M. Bentsen, I. Bethke, M. Ilicak, K. M. Assmann, and C. Heinze (2016), Evaluation of NorESM-OC (versions 1 and 1.2), the ocean carbon-cycle stand-alone configuration of the Norwegian Earth System Model (NorESM1), *Geosci. Model Dev.*, *9*(8), 2589-2622.

Séférian, R., et al. (2019), Evaluation of CNRM Earth System Model, CNRM-ESM2-1: Role of Earth System Processes in Present-Day and Future Climate, *Journal of Advances in Modeling Earth Systems*, *11*(12), 4182-4227.

Smith, L. M., and J. T. Andrews (2000), Sediment characteristics in iceberg dominated fjords, Kangerlussuaq region, East Greenland, *Sediment Geol*, *130*(1), 11-25.

Solan, M., E. R. Ward, E. L. White, E. E. Hibberd, C. Cassidy, J. M. Schuster, R. Hale, and J. A. Godbold (2019), Worldwide measurements of bioturbation intensity, ventilation rate, and the mixing depth of marine sediments, *Sci Data*, *6*(1), 58. DOI:10.1038/s41597-019-0069-7.

Song, S., et al. (2022), A global assessment of the mixed layer in coastal sediments and implications for carbon storage, *Nat Commun*, *13*(1), 4903.

Souchez, R., L. Janssens, M. Lemmens, and B. Stauffer (1995), Very-Low Oxygen Concentration in Basal Ice from Summit, Central Greenland, *Geophys Res Lett*, *22*(15), 2001-2004.

Stock, C. A., J. P. Dunne, S. Fan, P. Ginoux, J. John, J. P. Krasting, C. Laufkötter, F. Paulot, and N. Zadeh (2020), Ocean Biogeochemistry in GFDL's Earth System Model 4.1 and Its Response to Increasing Atmospheric CO2, *Journal of Advances in Modeling Earth Systems*, *12*(10), e2019MS002043.

Torres, M. A., A. J. West, and G. Li (2014), Sulphide oxidation and carbonate dissolution as a source of CO2 over geological timescales, *Nature*, *507*(7492), 346-349.

Treat, C. C., A. A. Bloom, and M. E. Marushchak (2018), Nongrowing season methane emissions–a significant component of annual emissions across northern ecosystems, *Global Change Biology*, *24*(8), 3331-3343.

Urakawa, L. S., H. Tsujino, H. Nakano, K. Sakamoto, G. Yamanaka, and T. Toyoda (2020), The sensitivity of a depth-coordinate model to diapycnal mixing induced by practical implementations of the isopycnal tracer diffusion scheme, *Ocean Modelling*, *154*, 101693.

Verbeke, V., R. Lorrain, S. J. Johnsen, and J.-L. Tison (2002), A multiple-step deformation history of basal ice from the Dye 3 (Greenland) core: new insights from the CO2 and CH4 content, *Annals of Glaciology*, *35*, 231-236.

Wang, Q., S. Danilov, D. Sidorenko, R. Timmermann, C. Wekerle, X. Wang, T. Jung, and J. Schröter (2014), The Finite Element Sea Ice-Ocean Model (FESOM) v.1.4: formulation of an ocean general circulation model, *Geosci. Model Dev.*, *7*(2), 663-693.

Ward, B. B., K. A. Kilpatrick, A. E. Wopat, E. C. Minnich, and M. E. Lidstrom (1989), Methane oxidation in Saanich inlet during summer stratification, *Cont Shelf Res*, *9*(1), 65-75.

Watanabe, E., M. Jin, H. Hayashida, J. Zhang, and N. Steiner (2019), Multi-Model Intercomparison of the Pan-Arctic Ice-Algal Productivity on Seasonal, Interannual, and Decadal Timescales, *Journal of Geophysical Research: Oceans*, *124*(12), 9053-9084.

Wik, M., R. K. Varner, K. W. Anthony, S. MacIntyre, and D. Bastviken (2016), Climate-sensitive northern lakes and ponds are critical components of methane release, *Nat Geosci*, *9*(2), 99-105.

Willerslev, E., et al. (2007), Ancient biomolecules from deep ice cores reveal a forested Southern Greenland, *Science*, *317*(5834), 111-114.

Wright, R. M., C. Le Quéré, E. Buitenhuis, S. Pitois, and M. J. Gibbons (2021), Role of jellyfish in the plankton ecosystem revealed using a global ocean biogeochemical model, *Biogeosciences*, *18*(4), 1291-1320.